Bachelor Thesis

Czech
Technical
University
in Prague

F3

Faculty of Electrical Engineering
Department of Control Engineering

Analysis of vehicle components and their impact on lap-time

Richard Ciglanský

Supervisor: doc. Ing. Tomáš Haniš Ph.D.
May 2024

BACHELOR'S THESIS ASSIGNMENT

I. Personal and study details

Student's name: **Ciglanský Richard** Personal ID number: **498930**

Faculty / Institute: **Faculty of Electrical Engineering**

Department / Institute: **Department of Control Engineering**

Study program: **Cybernetics and Robotics**

II. Bachelor's thesis details

Bachelor's thesis title in English:

Analysis of vehicle components and their impact on lap-time

Bachelor's thesis title in Czech:

Analýza vlivu komponent vozu na traťový čas

Guidelines:

1. Get familiar with vehicle components suitable for Formula Student vehicle.
2. Get familiar with vehicle dynamics, mathematical model of vehicle components and develop suitable model for lap-time analysis.
3. Prepare simulation and optimization framework for Formula Student competition, including relevant racing tracks, vehicle dynamics and considered components.
4. Perform vehicle performance analysis based on optimization framework.
5. Vehicle performance verification using high-fidelity vehicle dynamics simulations, like IPG CarMaker.

Bibliography / sources:

[1] Dieter Schramm, Manfred Hiller, Roberto Bardini – Vehicle Dynamics – Duisburg 2014
[2] Hans B. Pacejka - Tire and Vehicle Dynamics – The Netherlands 2012
[3] Robert Bosch GmbH - Bosch automotive handbook - Plochingen, Germany : Robet Bosch GmbH ; Cambridge, Mass. : Bentley Publishers
[4] J. A. E. Andersson, J. Gillis, G. Horn, J. B. Rawlings, and M. Diehl, “CasADi – A software framework for nonlinear optimization and opti- mal control,” Mathematical Programming Computation, vol. 11, no. 1, pp. 1–36, 2019.

Name and workplace of bachelor's thesis supervisor:

doc. Ing. Tomáš Haniš, Ph.D. Department of Control Engineering FEE

Name and workplace of second bachelor's thesis supervisor or consultant:

Date of bachelor's thesis assignment: **02.02.2024** Deadline for bachelor thesis submission: **24.05.2024**

Assignment valid until:
by the end of summer semester 2024/2025

doc. Ing. Tomáš Haniš, Ph.D. Supervisor's signature	prof. Ing. Michael Šebek, DrSc. Head of department's signature	prof. Mgr. Petr Páta, Ph.D. Dean's signature

III. Assignment receipt

The student acknowledges that the bachelor's thesis is an individual work. The student must produce his thesis without the assistance of others, with the exception of provided consultations. Within the bachelor's thesis, the author must state the names of consultants and include a list of references.

.

Date of assignment receipt	Student's signature

Acknowledgements

I would like to thank doc. Ing. Tomáš Haniš, Ph.D., for helping me understand vehicle dynamics from different points of view and for keeping me on the correct path to solve the problems. I want to express my gratitude to team eForce Prague Formula for exposing me to various challenges faced by motorsports teams and for the opportunity to work on them.

Declaration

I declare that this work is all my own work and I have cited all sources I have used in the bibliography.

Prague, May 19, 2024

Abstract

This thesis evaluates the impact on the lap time of torque vectoring, rear wheel steering and ground effect production device. To achieve this, the thesis presents a framework to calculate lap time for vehicles. The optimisation framework developed by Ing. Martin Gurtner, Ph.D. has been expanded by adding a more refined twin track model, suspension, aerodynamics, powertrain, tire model and torque vectoring. This framework uses CasADi [1] to define the optimal control problem and Ipopt [2] to solve it. The vehicle model has been validated using real driving data. The impact of systems has been analysed and verified using CarMaker simulation. The framework developed in this thesis can be used to perform sensitivity analysis of vehicle parameters on lap time and assist with further development of Formula Student vehicle by eForce Prague Formula.

Keywords: lap time simulation, Formula Student, Optimal Control, CasADi, Ipopt, Matlab, torque vectoring

Supervisor: doc. Ing. Tomáš Haniš Ph.D.
Prague 2, Karlovo náměstí, 13E

Abstrakt

Táto bakalárska práca hodnotí vplyv vektorovania krútiaceho momentu, riadenia natočenia zadných kolies a zariadenia na produkciu ground effectu na čas na kolo. Na dosiahnutie tohto cieľa práca predstavuje toolbox na výpočet času na kolo. Optimalizačný toolbox, ktorý vyvinul Ing. Martin Gurtner, Ph.D. bol rozšírený pridaním zdokonalenejšieho dvojstopého modelu, odpruženia, aerodynamiky, pohonneho retazcu, modelu pneumatík a vektorovania krútiaceho momentu. Tento toolbox využíva CasADi [1] na definovanie problému optimálneho riadenia a Ipopt [2] na jeho riešenie. Model vozidla bol overený na reálnych jazdných dátach. Vplyv systémov bol analyzovaný a overený pomocou simulácie CarMaker. Toolbox vyvinutý v tejto práci môže byť použitý na vykonanie citlivostnej analýzy parametrov vozidla na čas na kolo a pomôcť pri ďalšom vývoji vozidla Formula Student tímu eForce Prague Formula.

Klíčová slova: simulace traťového času, Formula Student, Optimálne Riadenie, CasADi, Ipopt, Matlab, vektorovanie momentu

Překlad názvu: Analýza vlivu komponent vozu na traťový čas

Contents

Figures

Tables

Chapter 1
Introduction

1.1 Motivation

The goal of the Formula Student competition is to design a car, manufacture it and drive 4 disciplines in the least amount of time. To make the fastest car the designers need to find out which systems e.g. torque vectoring, rear steering or GEPD the car should have, which aspects of the vehicle should be changed, and which not. Due to limited resources, the designers are always dealing with compromises when deciding on which systems to implement and what parameters the vehicle should have. One example is that increasing accumulator capacity allows the vehicle to use more energy and be faster on one discipline but it also increases the mass. Mass negatively impacts all disciplines. Designers need to know whether the gain from increasing the capacity will surpass the loss from increased mass. The toolbox in this thesis aims to help vehicle designers decide which systems the car should have. It should also help with identifying which parameters have the highest impact on lap time and how much effort should be put into changing those parameters e.g. reducing mass, moment of inertia, drag ...

Another requirement for completing the laps in the shortest amount of time is the actuating of the wheels. Traditionally only torque on one axle and steering of the front wheels is controlled. However, a wheel can be actuated in all 6 degrees of freedom. Determining how lap time is influenced when some of these DOF are actuated, allows designers to make informed decisions, about which DOF are worth actuating. Wheel DOF which are commonly actuated by Formula Student Vehicles are: driving torque on each wheel (Torque Vectoring) and steering of each wheel. Therefore only torque vectoring and rear steering are analyzed in this thesis. This work aims to quantify by how many seconds optimal torque vectoring and optimal all-wheel steering decrease the lap time. This should also help with understanding the systems and future controller design.

A new system this year is a ground effect production device, this device creates downforce by pulling air from underneath the vehicle. This work aims to quantify the decrease in lap time by this device and how to control this device, as it has limited accumulator capacity and cannot be activated all the time.

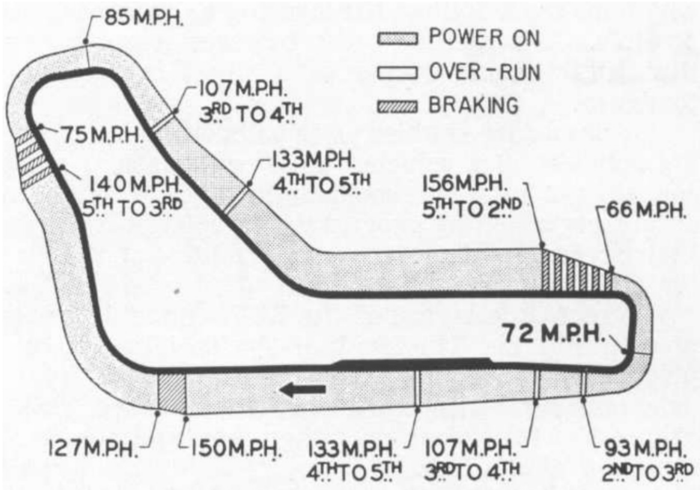

Figure 1.1: Analysis of Monza circuit in Italy

1.2 State of the art of Minimum lap time simulations (MLTS)

The purpose of MLTS is to find the minimum time for a vehicle to complete a lap, which leads to optimal control problem. Lap time simulations can be used for sensitivity analysis of vehicle parameters, evaluation of control strategies, and setup of vehicle for a specific track. Early attempts to compute lap-time, shift and braking points started in the 1950s[4][5], for example, the calculation for Monza Italy in figure 1.1. Early use of the steady state computer simulation is mentioned in 1971 [6], where performance envelope [7] and predefined trajectory were used. The approach of solving MLTS using optimal control methods appeared in 1992 [8], where a 3 DOF single track model is considered and the optimizer determines the trajectory. The input variables of optimization are torque on the front wheel, torque on the rear wheel, steering angle on the front and rear wheel. The objective is time and constraints are created by vehicle model and track. The twin track model is considered in [9] from 1996. Seven DOF vehicle model is employed in [10], which includes longitudinal, lateral, yaw motions of car chassis and the spin of each wheel. In [11] chassis with six DOF, suspension travel for each wheel and wheel spin is considered which considers a 14 DOF model. An electric vehicle with 4 independent motors is considered in [12].

The simplest method of solving MLTS is a steady state simulation, it can be done in Microsoft Excel. It works by parametrising the vehicle by its performance envelope [7], track is often fixed trajectory. Steady state method is used in [6].Example of free software using this method is OptimumLAP [13]. Motor sport teams use this method widely. The main advantage is its simplicity, disadvantages are that track, wheelbase, TV, limiting energy consumed, transient dynamics, etc. are difficult to simulate using this method.

Another method commonly used to solve MLTS is a transient method, which often uses nonlinear optimisation. Implementations of this method use single or twin track model and allow more complex models of vehicle systems than steady state simulations. A good source on the state of the art of lap time simulation and history is [5].

Chapter 2

Formula Student Competition

This section introduces the competition and how points are scored. Formula Student competition has dynamic and static events, for this thesis, only dynamic events are relevant, namely: Endurance, Autocross, Skidpad, and Acceleration. Each event has different maximum number of points see table 2.1. In this thesis, Formula Student Czech 2023 is considered.

Discipline	Acceleration	Skidpad	Autocross	Endurance
Points	50	50	100	250

Table 2.1: Points of disciplines

2.1 Skidpad

Skidpad is a discipline designed to test the steady state lateral characteristics of the vehicle. The skidpad track is depicted in figure 2.1. The pilot drives 2 full laps on the right circle, then 2 laps on the left circle. The second lap on each side is measured and times are averaged. Points are awarded according to the equation

$$Points_{Skidpad} = 46.5\left(\frac{\left(\frac{T_{max}}{T_{team}}\right)^2 - 1}{0.5625}\right) + 3.5. \tag{2.1}$$

T_{team} is the time of team
T_{max} is 1.25 times the time of the fastest vehicle

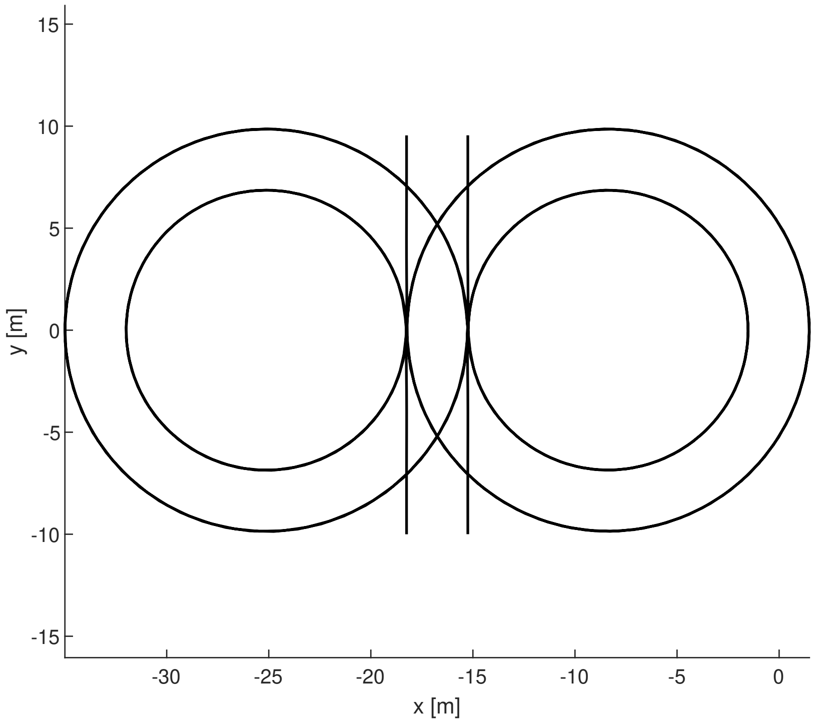

Figure 2.1: Skidpad track

2.2 Acceleration

Acceleration tests longitudinal characteristics of the vehicle. The acceleration track is a 75m straight line at least 3m wide. Points are awarded according to the equation

$$Points_{Acceleration} = 46.5 \left(\frac{\left(\frac{T_{max}}{T_{team}}\right) - 1}{0.5} \right) + 3.5. \qquad (2.2)$$

T_{team} is the time of team
T_{max} is 1.25 times the time of the fastest vehicle

2.3 Autocross

Autocross is a single lap around a track around 1 km long. The track is depicted in figure 2.2. The track layout has been obtained from GPS driving data. Points are awarded according to equation 2.3. This discipline is focused on testing the combined lateral, longitudinal and dynamic characteristics.
T_{team} is the time of team
T_{max} is 1.25 times the time of the fastest vehicle

$$Points_{Autocross} = 95.5 \left(\frac{\left(\frac{T_{max}}{T_{team}}\right) - 1}{0.25} \right) + 4.5 \qquad (2.3)$$

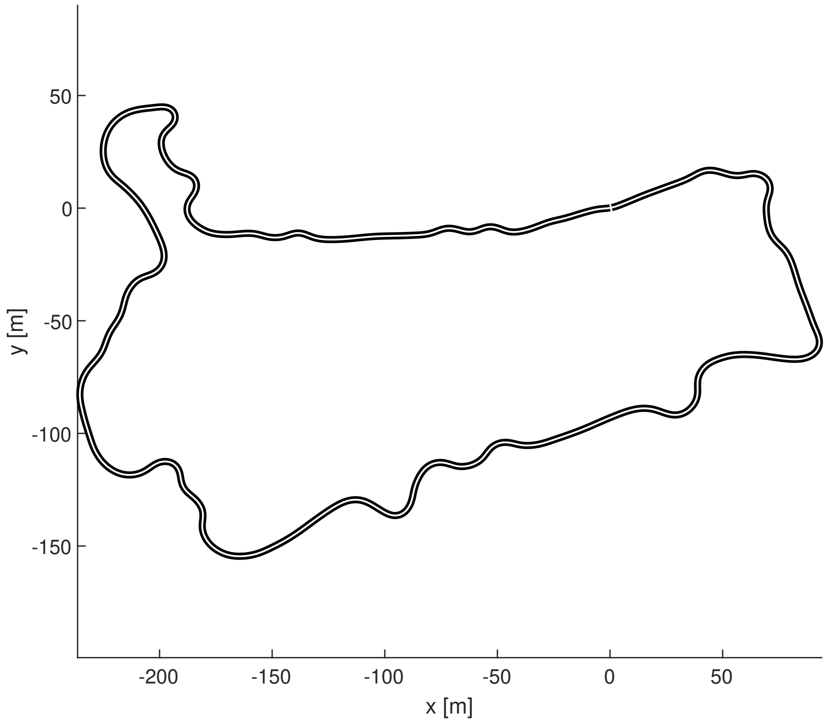

Figure 2.2: Formula Student Czech track

2.4 Endurance

Endurance is 22 laps around usually the same track as autocross track from figure 2.2. This discipline is focused on testing the same characteristics as autocross and adds reliability, pilot factor and energy consumption. Points are awarded according to equation

$$Points_{Endurance} = 225 \left(\frac{\left(\frac{T_{max}}{T_{team}}\right) - 1}{0.333} \right) + 22.5. \tag{2.4}$$

T_{team} is the time of team
T_{max} is 1.25 times the time of the fastest vehicle

2.5 Efficiency

Efficiency is measured during endurance discipline. The efficiency score is calculated by the equation

$$Points_{Efficiency} = 75 \left(\frac{EF_{max} - EF_{team}}{EF_{max} - EF_{min}} \right). \tag{2.5}$$

$EFteam$ the team's efficiency factor
$EFmin$ the lowest efficiency factor of all teams

$EFmax$ is defined as $1.5 \cdot EFmin$
The efficiency factor of a team is calculated by the equation:

$$EF = T^2 \cdot E. \tag{2.6}$$

where
T is driving time
E is used energy

Chapter 3

Formula Student modelling

Formula student vehicles are built to compete in Formula student competition. Average speed on endurance is around 60 km/h, speeds exceeding 100 km/h are rarely achieved during endurance discipline. In general, Formula Student tracks have few straights and many turns, therefore Formula Student vehicles are designed for high accelerations and relatively low top speeds. Histograms of speed and combined acceleration on figure 3.2a and 3.2b are taken from FSCZ competition driving data.

The vehicle can be separated into 4 systems: Suspension, Powertrain, Chassis and Aerodynamics. This chapter describes the systems and how they are modelled. In this thesis, vehicle CTU24 3.1 by eForce Prague Formula is considered, which has not yet been built at the time of writing. There are

Figure 3.1: Formula Student Vehicle CTU24

numerous ways to describe the behaviour of a vehicle. The simplest model is a mass point which accelerations are limited by performance envelope [7], this is used by steady state lap-time simulations. A more complex model is the singletrack model, where the vehicle is simplified to a bicycle.

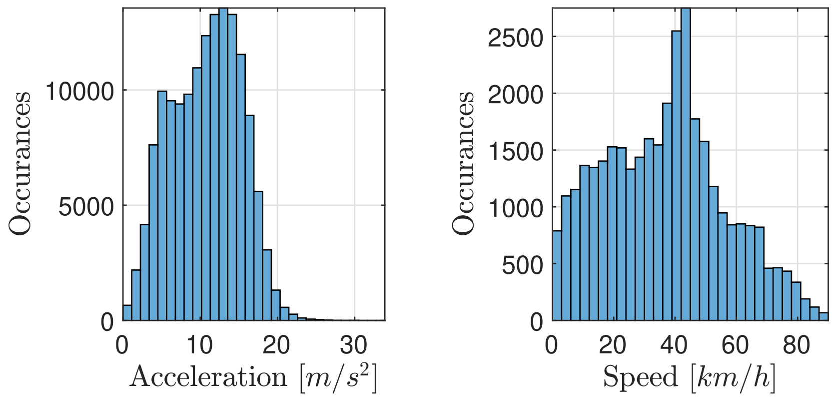

(a) : Acceleration Histogram FSCZ

(b) : Histograms FSCZ

Figure 3.2: FSCZ Endurance data histograms

3.1 Tire modeling

Most forces that govern vehicle movement are transferred by the tires. The tire is considered to be the most important system of a vehicle and the most difficult system to simulate [14]. Thus they need to be modeled with great caution in mind. Not only are there many parameters, such as tire wear, tire temperature, road friction, tire pressure, etc., that affect the resultant forces, they are also constantly changing during the lap. Therefore they are difficult to measure and model precisely.

There are four approaches to modelling tires depicted in figure 3.3. Models in this thesis are using the similarity method. They consider tires to be a source of lateral and longitudinal forces. Longitudinal force is usually modelled as a function of slip ratio λ. Model used in the optimisation framework is not considering the spin of wheels as that would increase the complexity of the mode, therefore slip ratio cannot be modelled. The lateral force is modeled as a function of slip angle α and normal load on tire F_z. Slip angle is the angle between the direction the tire is pointing and where it is traveling, depicted in figure 3.4 and equation

$$\alpha = -\arctan\left(\frac{v_y}{|v_x|}\right). \tag{3.1}$$

Slip ratio is calculated in equation

$$\lambda = \frac{\omega \cdot radius}{v_x} - 1, \tag{3.2}$$

where ω is the angular velocity of a spinning tire. In reality, the tire forces are highly dependent on numerous other variables, such as camber [15], temperature, wear etc. which are not modelled. These were not modelled to keep the tire model relatively simple.

The tire model often used in the automotive industry is the Magic Formula tire model, where forces generated by the tire are modeled by equations 3.3

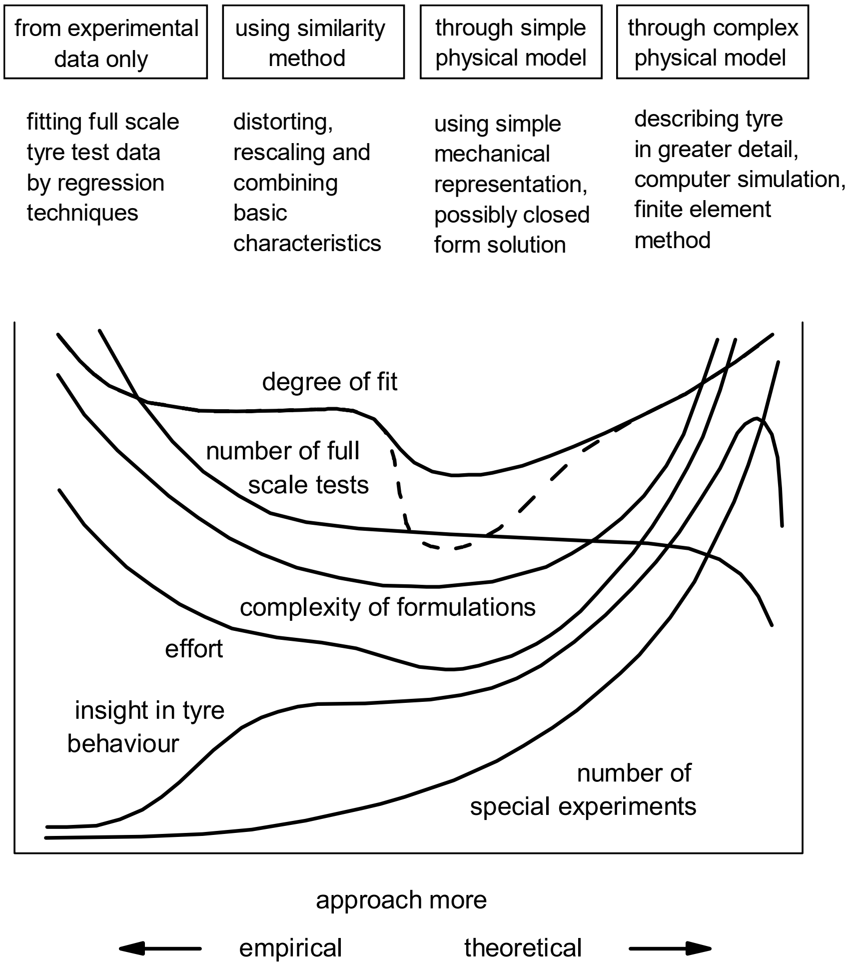

Figure 3.3: Four approaches of developing tire model[3]

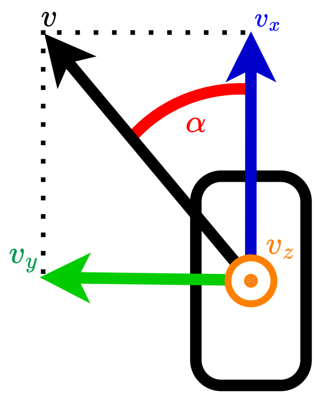

Figure 3.4: Tire diagram

and 3.4.

$$F_y = D_y \sin\left[C_y \arctan B_y \cdot \alpha - E_y(B_y \cdot \alpha - \arctan B_y \cdot \alpha)\right] \tag{3.3}$$

$$F_x = D_x \sin\left[C_x \arctan B_x \cdot \lambda - E_x(B_x \cdot \lambda - \arctan B_x \cdot \lambda)\right] \tag{3.4}$$

where A, B, C, D, E are fitted parameters.

3.1.1 Friction coefficients tire model

Tire forces are calculated using friction coefficients, maximal slip angle and tire normal force. Slip ratio is not considered. Inputs of the model are wheel slip angle α and tire normal force F_z. The output of this model is the maximal possible longitudinal force F_{xmax} and lateral force F_y. Parameters are lateral friction coefficient μ_y, longitudinal friction coefficient μ_x and maximal allowed slip angle α_{max}. The lateral force on a tire is calculated as:

$$F_{t_y} = \frac{\alpha}{\alpha_{max}} F_z \mu_y. \tag{3.5}$$

Forces are constrained by ellipse:

$$(\frac{F_{t_x}}{\mu_x})^2 + (\frac{F_{t_y}}{\mu_y})^2 \leq F_z^2. \tag{3.6}$$

This model does not consider the geometry of tire-road interaction as it would greatly increase the complexity of the simulation. The model is specially made for purpose of solving MLTS, as optimisation framework uses F_{t_x} on the tire as a decision variable which is constrained by equation 3.6 and by

$$-\alpha_{max} \leq \alpha \leq \alpha_{max}. \tag{3.7}$$

This makes sure the loss of traction which happens with real tire at α_{max} does not occur during simulation.

3.1.2 Tire testing and data

To find the relation between α, λ, F_z and generated forces, tires are tested on machines in figure 3.5. Tire data has been obtained from FSAE TTC [16]. Tire model has been parameterised so that it describes the force of tire until slip angle 5°, where the force levels off. Therefore $\alpha_{max} = 5°$.

Figure 3.5: Calspan tire testing machine

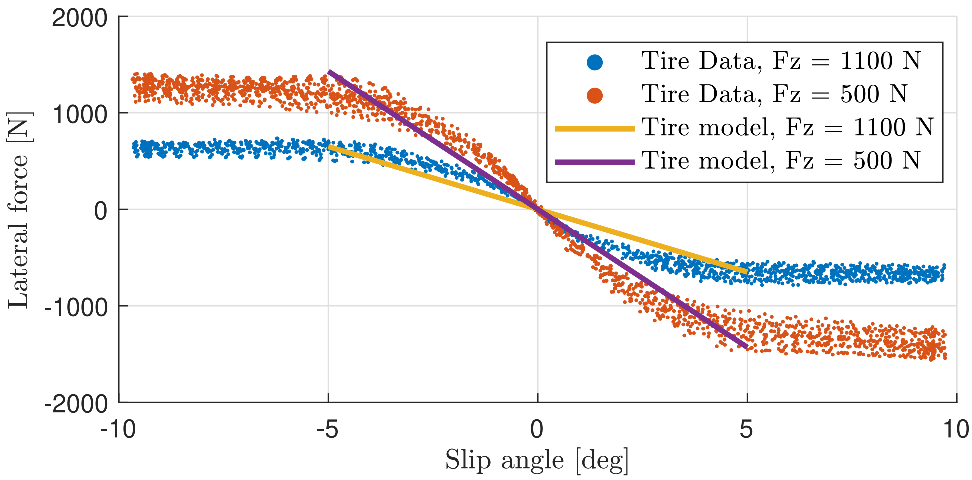

Figure 3.6: Comparison of tire data and tire model

3.2 Aerodynamic forces

The aerodynamic package trades the drag force for the normal force on tires. By increasing the normal force, tires can provide higher lateral and longitudinal force before losing grip. Formula Student vehicles usually have front, side and rear wings. The aerodynamic package of CTU24 is depicted in figure 3.7. The Aerodynamic package has a major impact on the normal force on tire, therefore they have a major impact on lap time too and should not be ignored.

Some formula student vehicles use a ground effect production device GEPD. This device uses high-power ducted fans to pull air from underneath the vehicle, thus amplifying the ground effect and creating additional normal force. However, this system adds additional weight. Forces generated by Aerodynamic package at constant speed can be approximated by the drag

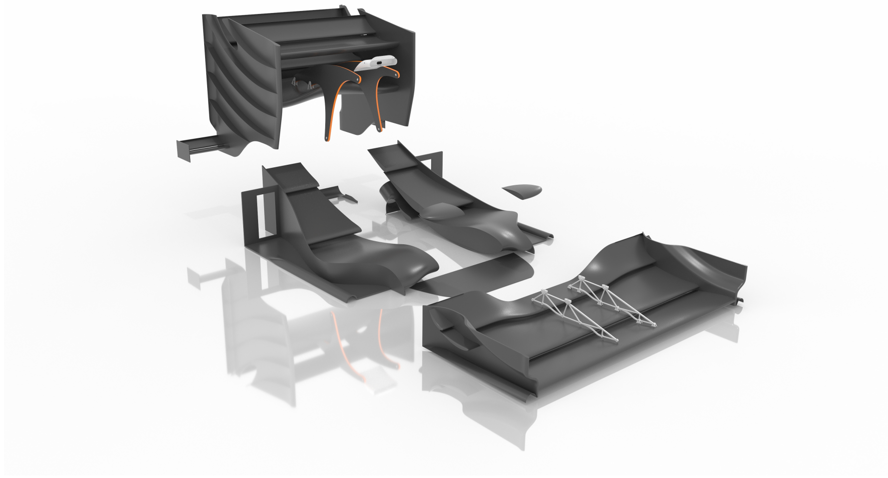

Figure 3.7: Aerodynamic package

equation [17]:

$$F_D = \frac{1}{2}\rho A C_D v_x^2, \tag{3.8}$$

$$F_L = \frac{1}{2}\rho A C_L v_x^2. \tag{3.9}$$

F_D is drag force and F_L is lift fore. C_d and C_L coefficients can be fitted from testing data or using computational fluid dynamics simulation.

3.3 Powertrain model

The powertrain of Formula Student vehicle consists of an accumulator, inverters, 4 motors, wiring, gearboxes, and hydraulic brakes. Braking is done using recuperating energy through motors and hydraulic brakes. Advantages of recuperation is that energy regenerated can be used again and the distribution of braking force is unrestricted. The disadvantage is the 30 kW recuperation power limit imposed by the accumulator. The advantage of hydraulic brakes is braking power which can exceed 200 kW. Disadvantages are that the energy is lost and the distribution of brake force between front and rear tires is constant. The best lap time is achieved by combining these two systems therefore they have to be modelled.

The powertrain model introduces five sources of force: hydraulic brake force F_{brake} and forces created by each motor $F_{motor n}$. Motor forces $F_{motor n}$ are limited by accumulator limits, motoring power limit P_{max}, generating power limit P_{min} as follows:

$$P_n = F_{motor n} \cdot v_{x t n}, \tag{3.10}$$

$$P_{loss_n} = |P_n| \cdot \eta, \tag{3.11}$$

$$P_{ACP} = \sum_{n=0}^{3} P_n + P_{n_{loss}}, \tag{3.12}$$

$$P_{min} \leq P_{ACP} \leq P_{max}. \tag{3.13}$$

Where η is the energy loss factor, $v_{x_{tn}}$ is the longitudinal speed of the tire in the tire frame, P_{loss_n} is power loss on each motor and P_{ACP} is total power flowing from the accumulator. Force on each motor is also limited by motor characteristics:

$$F_{motor_n} \leq F_{motor_{max}}, \tag{3.14}$$

where $F_{motor_{max}}$ is the maximum force current configuration of tire radius, gearbox ratio and motor can deliver. The hydraulic brake force is only limited by the forces the tire can deliver. The brake force on each tire is given by:

$$F_{brake\,FL} = \frac{F_{brake}}{2} \cdot (1 - BB), \tag{3.15}$$

$$F_{brake\,FR} = \frac{F_{brake}}{2} \cdot (1 - BB), \tag{3.16}$$

$$F_{brake\,RL} = \frac{F_{brake}}{2} \cdot BB, \tag{3.17}$$

$$F_{brake\,RR} = \frac{F_{brake}}{2} \cdot BB. \tag{3.18}$$

Where BB is brake balance; the distribution of hydraulic braking force between the front and rear tires. Force on n-th tire from the powertrain is defined by equation:

$$F_{x_n} = F_{motor_n} - F_{brake_n}. \tag{3.19}$$

Equation

$$\overrightarrow{P}_{ACP} \cdot \overrightarrow{\Delta t}^T \leq C_{ACP} \tag{3.20}$$

limits energy drawn during the race to that of accumulator capacity C_{ACP}. $\overrightarrow{P}_{ACP}$ stands for the vector of power drawn from the accumulator in each point of the simulation. $\overrightarrow{\Delta t}^T$ is a transposed vector of time spent between simulation points.

3.4 Suspension model

Suspension is responsible for utilizing the potential of the tire and for improving the handling of the vehicle. This is done by changing the geometry of tire-road interaction and normal load distribution between the tires. Suspension of Formula Student vehicles can be divided into 2 parts, kinematics and dynamics.

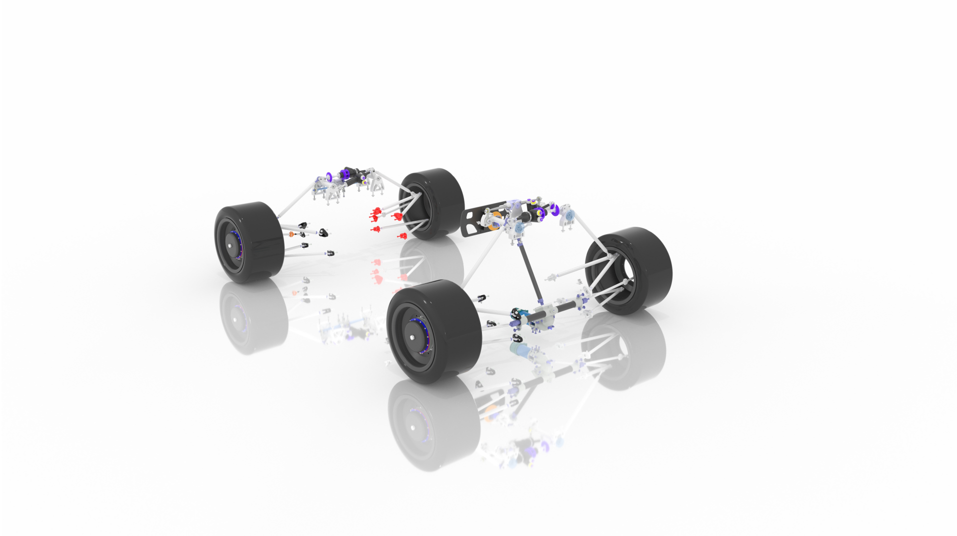

Figure 3.8: Suspension of CTU24

3.4.1 Suspension kinematics

Kinematics is the system that governs the geometry of tire-road interaction during wheel displacement (motion up and down) and steering. The geometry of tire-road interaction is complex and has a significant impact on the forces generated by the tire. The tire model does not consider geometry due to the large increase in model complexity. Therefore, the suspension model does not consider it either. Kinematics also define the coupling between roll, pitch and heave motions of the chassis figure 3.9.

Figure 3.9: Chassis of CTU24

The simplest kinematic system used by Formula Student teams is a fully coupled double wishbone. This means each wheel has separate damper and one spring. Using this system, it is not possible to change stiffness and damping in roll, pitch and heave (up and down motion) of the chassis independently, they are coupled.

A more complex kinematic system is a roll-heave decouple system, where the stiffness and damping in the roll of the chassis can be changed without changing the stiffness and damping in the heave and vice versa.

3.4.2 Load transfer

Suspension is responsible for handling the effects of load transfer [18]. Load transfer is used to describe the shifting of load on tires due to acceleration.

The suspension model considers wheels to be always touching the ground, wheel displacement is ignored. The suspension model models the lateral and longitudinal load transfer as first order systems. Load transferred is modelled by equations:

$$\dot{F}_{z_\Delta x} = \frac{F_x \frac{CoG_z}{b} - F_{z_\Delta x}}{t_{susx}}, \tag{3.21}$$

$$\dot{F}_{z_\Delta y} = \frac{F_y \frac{CoG_z}{b} - F_{z_\Delta y}}{t_{susy}}. \tag{3.22}$$

$F_{z_\Delta x}$ stands for the normal force added to the front axle and subtracted from the rear axle. $F_{z_\Delta y}$ stands for the normal force which is added to the left tires and subtracted from the right tires. t_{susx} t_{susy} are time constants of suspension dynamics.

3.5 GEPD model

GEPD model is characterised by parameters: power limit $P_{GEPDmax}$, maximum generated force $F_{GEPDmax}$, accumulator capacity C_{GEPD}, slew rate SR_{GEPD} and mass m_{GEPD}. GEPD force is limited by the equation:

$$0 \leq F_{GEPD} \leq F_{GEPDmax}. \tag{3.23}$$

Energy used by GEPD is limited by GEPD accumulator capacity

$$\overrightarrow{P}_{GEPD} \cdot \overrightarrow{\Delta t}^T \leq C_{GEPD}. \tag{3.24}$$

GEPD fans spin-up time is modeled by the equation:

$$\frac{\Delta F_{GEPD}}{\Delta t} \leq SR_{GEPD}. \tag{3.25}$$

There is a linear relation between force and power:

$$P_{GEPD} = \frac{F_{GEPD} P_{GEPDmax}}{F_{GEPDmax}}. \tag{3.26}$$

The normal force created by GEPD is distributed equally among wheels.

3.6 Twintrack model

Twintrack model builds a complete vehicle from the systems above. At first, velocities at tires must be calculated. This is done by creating the position and angular velocity vectors:

$$\vec{\omega} = \begin{bmatrix} 0 & 0 & \dot{\psi} \end{bmatrix}, \tag{3.27}$$

$$\vec{r} = \begin{bmatrix} l_i & \frac{b}{2} & 0 \end{bmatrix}, \tag{3.28}$$

where $\dot{\psi}$ is yaw rate, l_i is longitudinal distance of center of gravity from front and rear axle respectively. Velocities at tire pivot points $\vec{v_{p_i}}$ are calculated as:

$$\vec{v_{p_i}} = \vec{v} + \vec{\omega} \times \vec{r_i}. \tag{3.29}$$

Velocities are transformed from pivot frame to tire frame:

$$R_t = \begin{bmatrix} \cos\delta_i & -\sin\delta_i & 0 \\ \sin\delta_i & \cos\delta_i & 0 \\ 0 & 0 & 0 \end{bmatrix}, \tag{3.30}$$

$$\vec{v_{ti}} = \vec{v_{p_i}} R. \tag{3.31}$$

Vector $\vec{v_{ti}}$ contains velocities of tire in tire frame

$$\vec{v_{ti}} = \begin{bmatrix} v_{xt_i} \\ v_{yt_i} \\ v_{zt_i} \end{bmatrix}. \tag{3.32}$$

tire forces F_{tx} and F_{ty} are calculated by equation 3.5. Then, forces are transformed back to the pivot frame:

$$\begin{bmatrix} F_{x_i} \\ F_{y_i} \end{bmatrix} = \begin{bmatrix} \cos\delta_i & \sin\delta_i \\ -\sin\delta_i & \cos\delta_i \end{bmatrix} \begin{bmatrix} F_{t_x} \\ F_{t_y} \end{bmatrix}. \tag{3.33}$$

Controls of the model are in table 3.1, states are in table 3.2

$\vec{u}$	Controls	Units
δ_f	Front wheels steering	rad
δ_f	Rear wheels steering	rad
F_{xFL}	Force produced by front left motor	N
F_{xFR}	Force produced by front right motor	N
F_{xRL}	Force produced by rear left motor	N
F_{xRR}	Force produced by rear right motor	N
$F_{x_{brake}}$	Force produced by brakes	N
F_{GEPD}	Force produced by GEPD	N

Table 3.1: Controls

$\vec{z}$	States	Units
v_x	Velocity along vehicle X axis	m/s
v_y	Velocity along vehicle Y axis	m/s
ψ	Heading of vehicle	rad
$\dot{\psi}$	Yaw rate	rad/s
n	Position perpendicular to center line	m
t	Time	s
$F_{z\Delta x}$	Load transfer on front wheels	F
$F_{z\Delta y}$	Load transfer on front wheels	F

Table 3.2: States

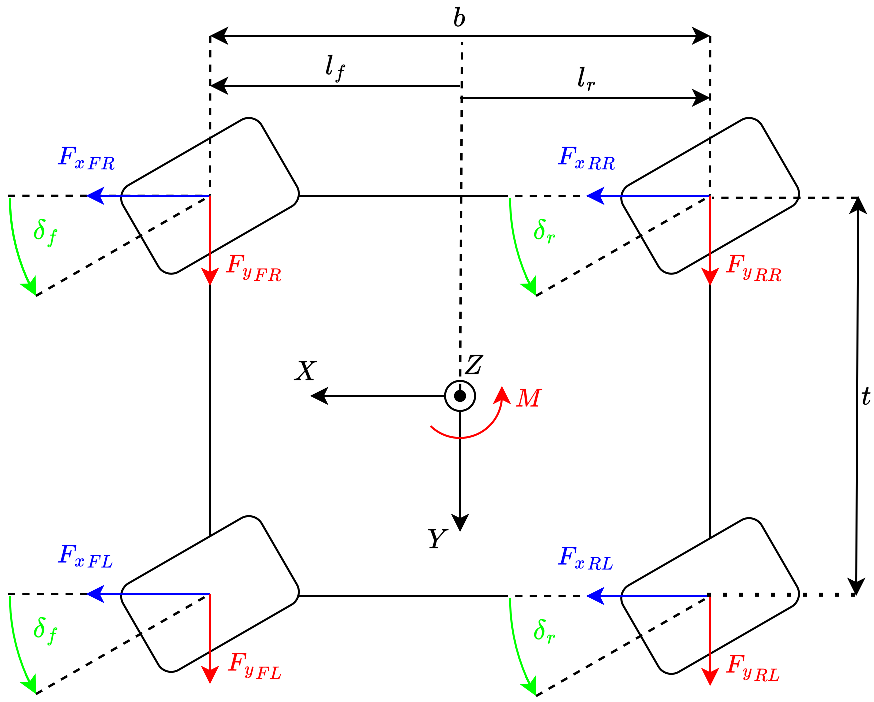

Figure 3.10: Twin track diagram

Forces created by tires are depicted in figure 3.10. Derivations of states in respect to time are defined by equations:

$$F_x = F_{xFL} + F_{xFR} + F_{xRL} + F_{xRR} - F_D, \tag{3.34}$$

$$F_y = F_{yFL} + F_{yFR} + F_{yRL} + F_{yRR}, \tag{3.35}$$

$$M = (-F_{xFL} + F_{xFR} - F_{xRL} + F_{xRR})\frac{t}{2} + (F_{yFR} + F_{yFL})l_f - (F_{yRR} + F_{yRL})l_r, \tag{3.36}$$

$$\dot{v_x} = \frac{F_x}{m} + \dot{\psi}v_y, \tag{3.37}$$

$$\dot{v_y} = \frac{F_y}{m} - \dot{\psi}v_x, \tag{3.38}$$

$$\ddot{\psi} = \frac{M}{I}, \tag{3.39}$$

$$\dot{F}_{z_{\Delta}x} = \frac{F_x \frac{CoG_z}{b} - F_{z_{\Delta}x}}{t_{sus}}, \tag{3.40}$$

$$\dot{F}_{z_{\Delta}y} = \frac{F_x \frac{CoG_z}{b} - F_{z_{\Delta}y}}{t_{sus}}. \tag{3.41}$$

3.7 Carmaker model

Carmaker is multi-body simulation software developed by IPG Automotive. It is widely used in the automotive industry for testing autonomous vehicles, vehicle dynamics, powertrains, and advanced driver assistance systems. To validate the twintrack model, a Formula Student vehicle model has been created using Carmaker and validated for lateral steady state characteristics.

3.8 Model validation

Model used by optimisation framework has to be validated before the results can be used in any application. The best way to validate a model is to compare it with data from real car testing. The twin track model has been validated using the Carmaker model and real car driving data. The maneuver used for validation is ramp steer, where speed is constant and wheel angle is slowly increased to maximum. As CTU24 does not yet exist, the model was parameterized as formula model FSE11. Since the step steer was performed and measured with FSE11. In figure 3.11, a good match is shown between the model and measured data until the first tire reaches maximum slip angle at acceleration 13.8 m/s^2. At that point, the twin track model and reality diverge. The developed twin track model is a good representation of reality at v_x = 15 m/s until lateral acceleration reaches 13.8 m/s^2.

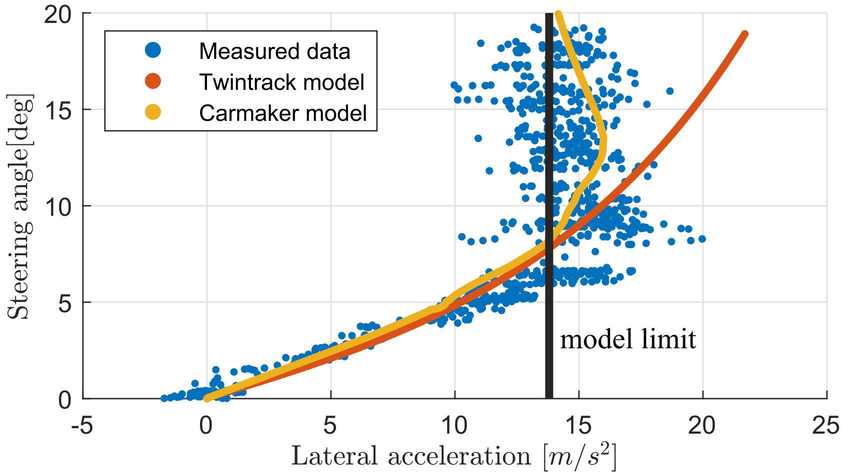

Figure 3.11: Ramp steer v = 15m/s

Mass (including pilot)	m	300	kg
Moment of Inertia (including pilot)	I	120	kgm^2
Track	t	1.2	m
Wheelbase	b	1.53	m
Mass distribution	CoGr	0.4876	-
CoG height	COGz	0.3	m
tire radius	r	0.205	m
Maximum steering angle front	$\delta_{f_{max}}$	25	deg
Maximum steering angle rear	$\delta_{r_{max}}$	6	deg
Steering slew rate	$\delta_{f_{maxRate}}$	100	deg/s
Gear ratio	gr	11.46	-
Maximum motor torque	T_{max}	29.1	Nm
Torque slew rate	SR_F	16000	Nm/s
Torque jerk	SR_F	800	Nm/s^2
Max Power	P_{max}	80	kW
Min Power	P_{min}	-30	kW
Accumulator Capacity	C_{AC}	7.4	kWh
Brake balance	BB	0.7	-
Powertrain losses	η	0.1	-
Longitudinal suspension constant	t_x	0.5	s
Lateral suspension constant	t_y	0.3	s
tire friction coefficient X	μ_x	1.5	-
tire friction coefficient Y	μ_y	1.3	-
tire maximum slip angle	α_{max}	5	deg
Lift coefficient	C_L	-4.15	-
Drag coefficient	C_D	1.55	-
Center of pressure ratio	COP_r	0.5	-
GEPD max power	$P_{GEPDmax}$	12	kW
GEPD max force	$F_{GEPDmax}$	882	N
GEPD accumulator capacity	C_{GEPD}	1.7	kWh
GEPD Force Slew rate	SR_{GEPD}	294	N/s
Font wing length	l_w	0.8	m

Table 3.3: CTU24 expected parameters

Chapter 4
Optimisation framework

This chapter describes how the optimisation problem was defined using CasADi syntax [1], solved by solver Ipopt [2]. CasADi is open-source tool for nonlinear optimization and algorithmic differentiation. It is implemented as toolbox in Matlab. Ing. Martin Gurtner, Ph.D. has created a framework to find the optimum controls for a single track model for a given track.

4.1 Problem discretization

The coordinate system used by the framework is three-dimensional: the first dimension is the position along the center line of the track, defined by points s, the second dimension is the distance of vehicle from the center line n; and the third dimension is the heading of vehicle ψ. Track is described by series of points, each point has X position, Y position and track heading θ. The coordinate system is depicted in figure 4.1. This kind of coordinate system is known in the literature as a curvilinear coordinate system [19]. It does not consider any change in elevation or banking. Derivation of states has

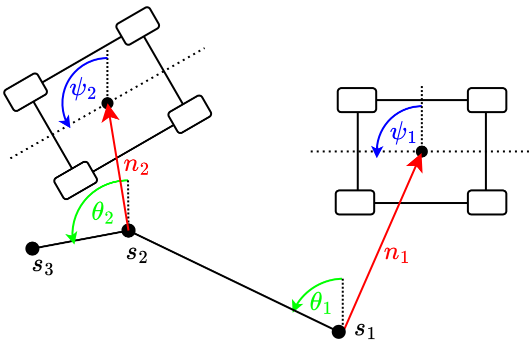

Figure 4.1: Coordinate system of optimisation framework

to be with respect to path s instead of time. Thus, the model developed in Chapter 3 has to be transformed from the time domain into the path domain. Optimization then solves the problem in the path domain instead of the time domain. Sampling distance of points has to be sufficiently small for the solver to find a solution. After the solution is found, the model is simulated in time with the controls transformed into time domain. Controls are applied in feed forward manner. This is done to verify that the time to path domain transformation was done correctly.

Decision variables of the solver are controls 3.1 and states 3.2, they are constrained by equations from the next chapter 4.2.

4.2 Constraints

Constraints are created using vehicle parameters, track, states and controls. They are defined by equations in tire model 3.5, powertrain model 3.14 3.13 3.20, GEPD model 3.24, 3.23, 3.25. Vehicle variants are also created using constraints. A vehicle with rear steering is made by constraint:

$$-6deg \geq \delta_r \leq 6deg. \tag{4.1}$$

while other variants are constrained by:

$$0 \geq \delta_r \leq 0. \tag{4.2}$$

A vehicle without torque vectoring is created by constraining motor forces:

$$F_{motor\,FL} = F_{motor\,FR}, \tag{4.3}$$

$$F_{motor\,RL} = F_{motor\,RR}. \tag{4.4}$$

Vehicle model is prevented from exceeding maximum slip angle α_{max} on any wheel by constraint

$$-\alpha_{max} \leq \alpha_n \leq \alpha_{max}. \tag{4.5}$$

Simulation of closed track where vehicle completes multiple laps around the same track is done by constraining end states to be the same as start states

$$\vec{z}_{end} = \vec{z}_1. \tag{4.6}$$

As the optimization is carried out in relation to the path, the constraint on time is required. Time has to start at zero and increase

$$t_n \geq 0. \tag{4.7}$$

To ensure the vehicle stays inside track, a hit-box has been created, equations limit the edges of the vehicle to stay inside the track:

$$\gamma_n = \theta_n - \psi_n, \tag{4.8}$$

$$-(r_l + l_w)\sin\gamma_n + T\cos\gamma_n + z_n \leq track\ width\ left, \tag{4.9}$$

$$-(f_l + l_w)\sin\gamma_n - T\cos\gamma_n - z_n \leq track\ width\ right, \tag{4.10}$$

$$-r_l\sin\gamma_n + T\cos\gamma_n + z_n \leq track\ width\ left, \tag{4.11}$$

$$-r_l \sin \gamma_n - T \cos \gamma_n - z_n \leq \textit{track width right}. \tag{4.12}$$

The simulation of the model in path is done by writing equations of 4th order Runge Kutta integration, which constrains the dynamics of the model:

$$\vec{k}_1 = f(s_n, \vec{z}_n, \vec{u}_n), \tag{4.13}$$

$$\vec{k}_2 = f\left(s_n + \frac{h}{2}, \vec{z}_n + \frac{\vec{k}_1}{2}h, \vec{u}_n\right), \tag{4.14}$$

$$\vec{k}_3 = f\left(s_n + \frac{h}{2}, \vec{z}_n + \frac{\vec{k}_2}{2}h, \vec{u}_n\right), \tag{4.15}$$

$$\vec{k}_4 = f\left(s_n + h, \vec{z}_n + h\vec{k}_3, \vec{u}_n\right), \tag{4.16}$$

$$\vec{z}_{n+1} = \vec{z}_n + \frac{h}{6}(\vec{k}_1 + 2\vec{k}_2 + 2\vec{k}_3 + \vec{k}_4). \tag{4.17}$$

Where $\vec{u}$ is the vector of controls 3.1 $\vec{z}$ is a vector of states 3.2, s is the position along the centerline, h is the step size and f is a function of twin track model.

4.3 Considerations

Additional constraints had to be added to prevent undesired oscillatory behavior. The rate of change of steering is constrained by the following:

$$-100 \leq \frac{\Delta \delta_f}{\Delta t} \leq 100. \tag{4.18}$$

The rate of change of longitudinal tire force is constrained by

$$-16000 \leq \frac{\Delta F_{xn}}{\Delta t} \leq 16000. \tag{4.19}$$

The second derivative of longitudinal tire force is constrained by

$$-800 \leq \frac{\Delta^2 F_{xn}}{\Delta t^2} \leq 800. \tag{4.20}$$

Solving the problem with the path as an independent variable makes it impossible to simulate a standstill as the vehicle never leaves the current point. Therefore, low speeds could not be simulated. This caused problems, particularly in the acceleration discipline.

Constraints have to be differentiable for the solver to find a solution. The equation for power loss 3.11 uses absolute value, which is not differentiable. To solve this, the absolute value is replaced by a differentiable approximation of the absolute value:

$$|x| \approx x \tanh x. \tag{4.21}$$

This change creates an error, depicted in Figure 4.2. The error is negligible.

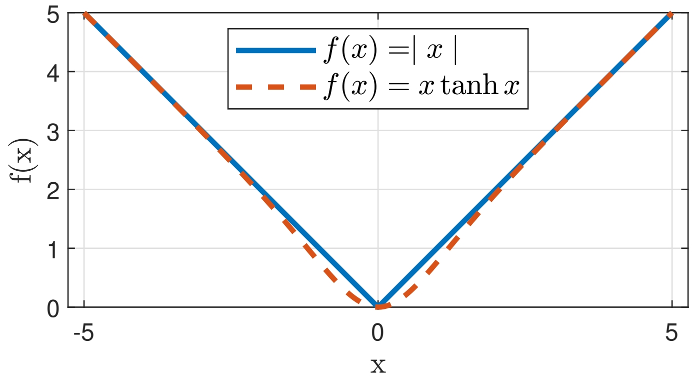

Figure 4.2: Absolute value approximation

4.4 Solver

The optimization objective is to minimize time. The solver requires an initial solution to start optimization. The initial solution is provided by driving the model around the track with P regulators on the steering and motor torque. The speed setpoint is set to a constant of 5m/s, and the path setpoint is the center line. The initial solution and constraints are passed to Ipopt [2], which returns a solution.

Chapter 5

Optimisation results

Four variants of a vehicle have been created: baseline, TV, RS and GEPD. Baseline vehicle is constrained by $F_{xFL} = F_{xFR}$ and $F_{xRL} = F_{xRR}$, effectively having one motor in front and one in the rear. TV has a motor in each wheel, each motor generates force independent of other motors. RS is a baseline car with the addition of rear wheel steering limited to 6 degrees. A vehicle with GEPD is a baseline car with the addition of a GEPD system, which also adds 10kg.

vehicle configuration	Torque Vectoring	Rear Steering	GEPD
baseline	no	no	no
TV	yes	no	no
RS	no	yes	no
GEPD	no	no	yes

Table 5.1: Vehicle variants

In this chapter, a simple analysis of each car's behavior in each discipline is performed, except acceleration, as TV and RS had no impact on acceleration. This analysis gives some insight into why systems reduced lap time, but further analysis is needed.

One of the metrics to evaluate vehicle performance is tire utilization. The idea behind tire utilization is to always be on the limit of the force a tire can create, so called tire ellipse defined by 3.6. tire utilization is calculated in equation 5.1, where n is number of samples.

$$Tire\ utilisation = \frac{1}{n}\sum_{1}^{n}\sqrt{\left(\frac{F_x}{F_z\mu_x}\right)^2 + \left(\frac{Fy}{F_z\mu_y}\right)^2}. \tag{5.1}$$

Induced tire drag is the lateral force created by the tire, which gets projected into longitudinal force by the steering angle

$$Induced\ tire\ drag = (F_{yFL} + (F_{yFR})\sin\delta_f + (F_{yRL} + (F_{yRR})\sin\delta_r. \tag{5.2}$$

Videos from simulations are available on YouTube

5.1 Impact of TV on lap-time

In this section impact of torque vectoring is investigated. All dynamic disciplines have been simulated with the vehicle with TV and compared to the baseline vehicle. In acceleration, the time was the same for both vehicles.

Vehicle	Acceleration	Skidpad	Autocross	Endurance	Overall
baseline	42.2	7.03	5.0324	113.15	167.65
TV	42.2	13.03	29.3	152.58	237.08
ΔTV	0	5.73	24.26	39. 12	69.42

Table 5.2: Points comparison between TV and baseline

5.1.1 Impact of TV on skidpad

To make the impact of the TV clear, only one left lap of the skidpad is shown. Figure 5.1 shows that the vehicle with TV has lower tire induced drag, lower steering angle and higher lateral acceleration compared to baseline. Figure 5.2 shows the longitudinal forces on wheels generated by motors. There is a higher force on right side of vehicle then on the left. Interesting fact is, that RR motor is braking and FR motor is accelerating the vehicle. This fact requires more investigation to determine the cause. The maneuver was left turn, inside tires were fully utilised by both vehicles, outside tires were better utilised by vehicle with TV, but not fully. During turn, the outside tires have larger normal force acting on them, therefore they can generate more lateral force, thus it is more important to fully utilise outside tires than inside tires. Average tire utilization for baseline was 0.9223, and for TV, 0.9664, which is a 4.58% difference.

Configuration	Time	Average Acceleration	Average speed	Points
baseline	5.06 s	11.87 m/s^2	9.53 m/s	7.3
TV	4.89 s	12.76 m/s^2	9.91 m/s	13.03
ΔTV	-0.16 s	0.88 m/s^2	0.37 m/s	5.73

Table 5.3: Time comparison baseline and TV

According to Table 5.3, torque vectoring improves the time on the skidpad by around 3.4% and adds 5.73 points to the score.

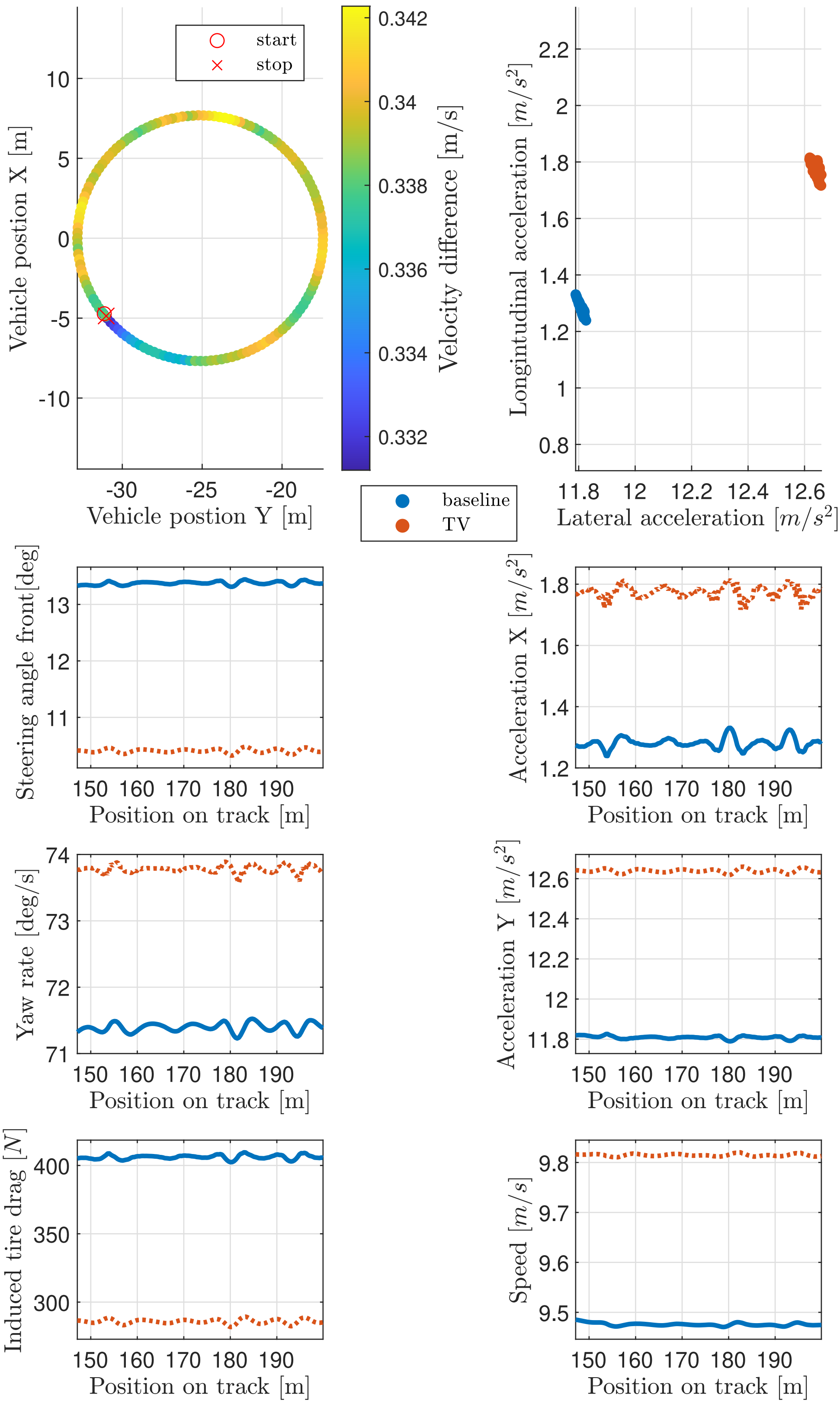

Figure 5.1: TV Skidpad analysis

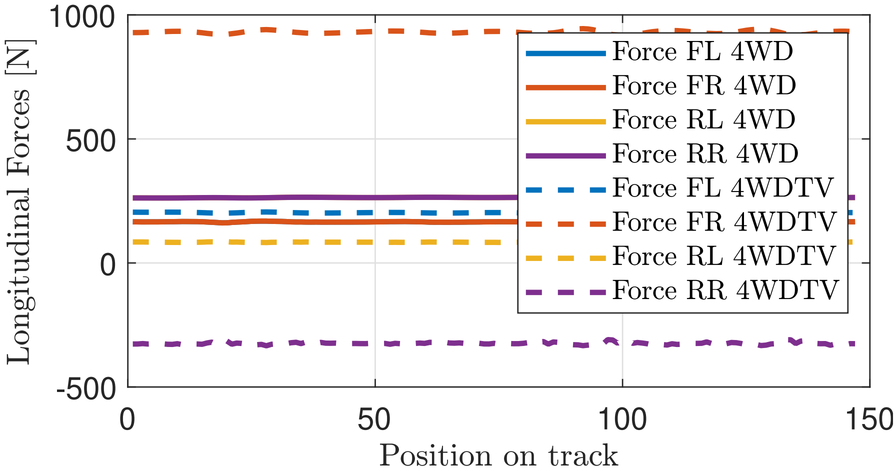

Figure 5.2: Longitudinal wheel forces on skidpad

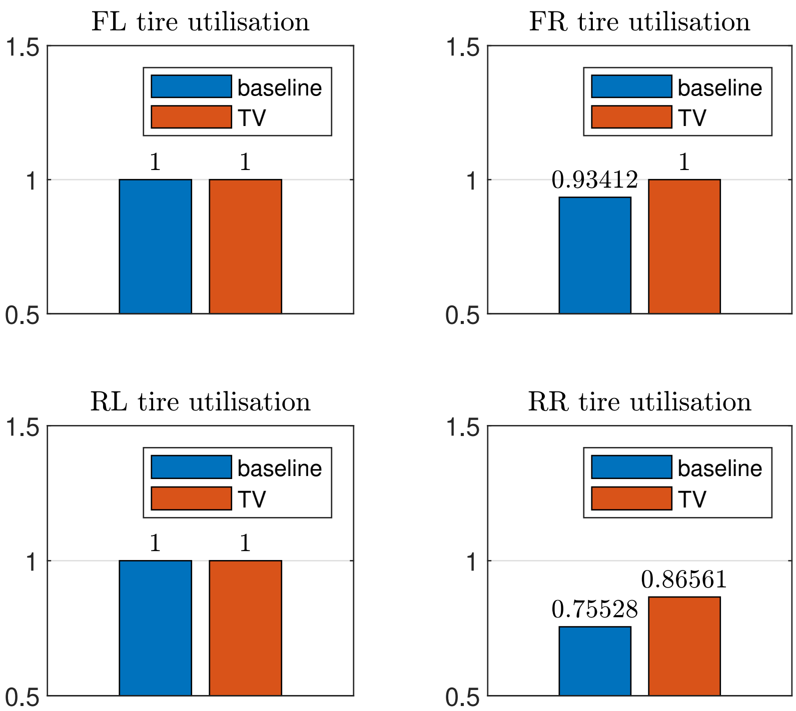

Figure 5.3: Tire utilisation of TV on Skidpad

5.1.2 Impact of TV on autocross

Analysis of the whole autocross would be impractical in this format. Therefore, a segment of the track is analyzed more thoroughly. Figure 5.5 depicts a segment of track which has acceleration braking, sharp and long turns, therefore it a good representation of the rest of track. From position 540 to 560, the vehicle with TV has almost zero resistances from steering and zero steering angle, and yet it has an almost constant yaw rate. Lower tire drag allows higher acceleration. On acceleration graphs, higher accelerations can be observed. Tire utilization figure 5.4 shows higher overall tire utilization for a vehicle with TV of 5.9%

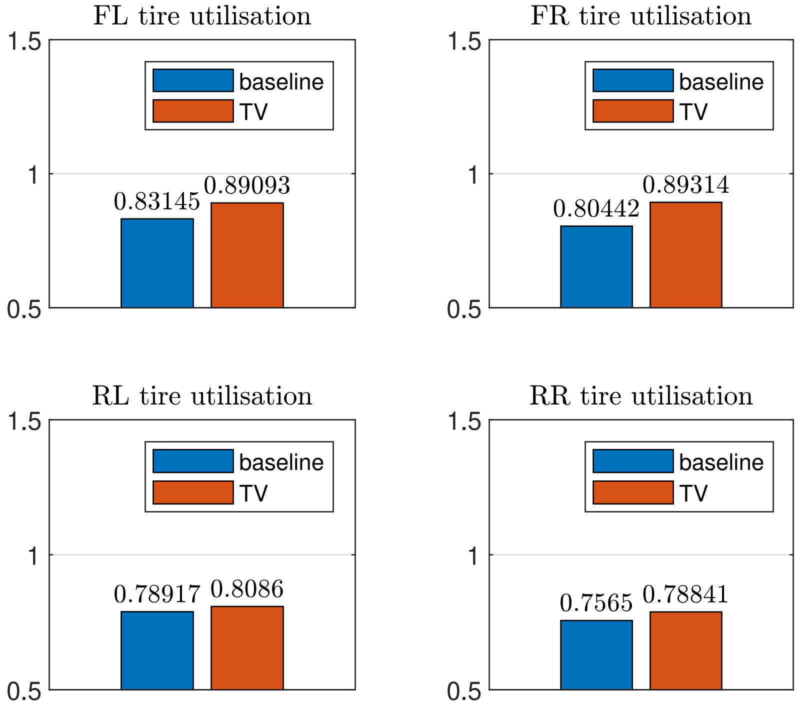

Figure 5.4: Tire utilization of TV on Autocross

Configuration	Time	Average Acceleration	Average speed	Points
baseline	65.74 s	12.23 m/s^2	16.60 m/s	5.03
TV	61.82 s	13.26 m/s^2	17.71 m/s	29.3
ΔTV	-3.92 s	1.03 m/s^2	1.10 m/s	24.27

Table 5.4: Time comparison baseline and TV on autocross

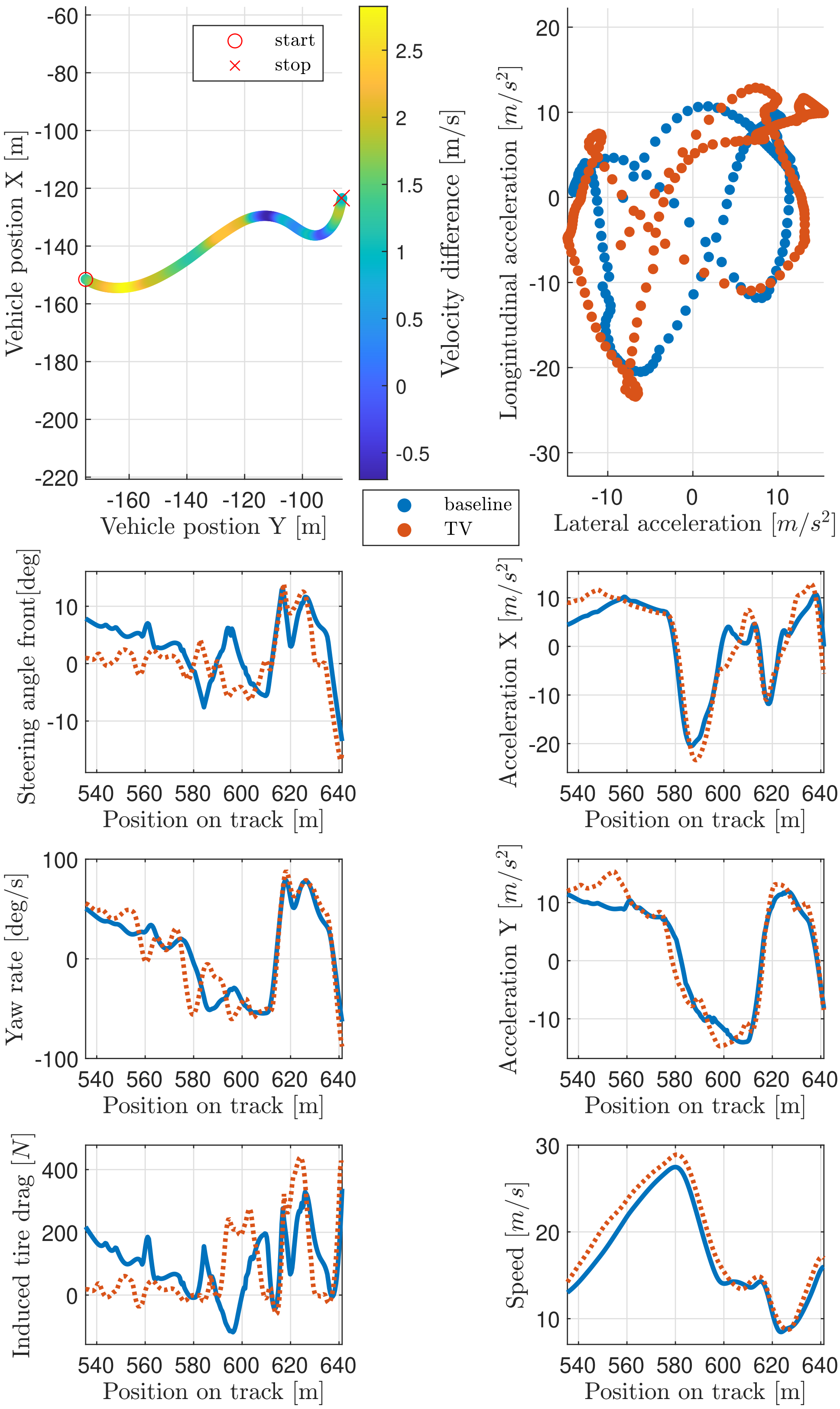

Figure 5.5: TV Autocross analysis

5.1.3 Impact of TV on endurance

Endurance is analysed on the same segment as autocross, the only difference between simulated endurance and simulated autocross is that energy for a lap is limited. On Figure 5.7 there are only small differences, vehicle with TV is slower from 570th to 590th meter and baseline in this case brakes harder than TV vehicle on 590th meter. Different from skidpad and autocross is the tire utilization, on endurance TV had lower tire utilization than baseline on figure 5.6. Overall tire utilisation is 1% lower on TV than on baseline, this could be due to the fact, that higher tire forces create higher tire drag and TV is avoiding this drag to preserve energy.

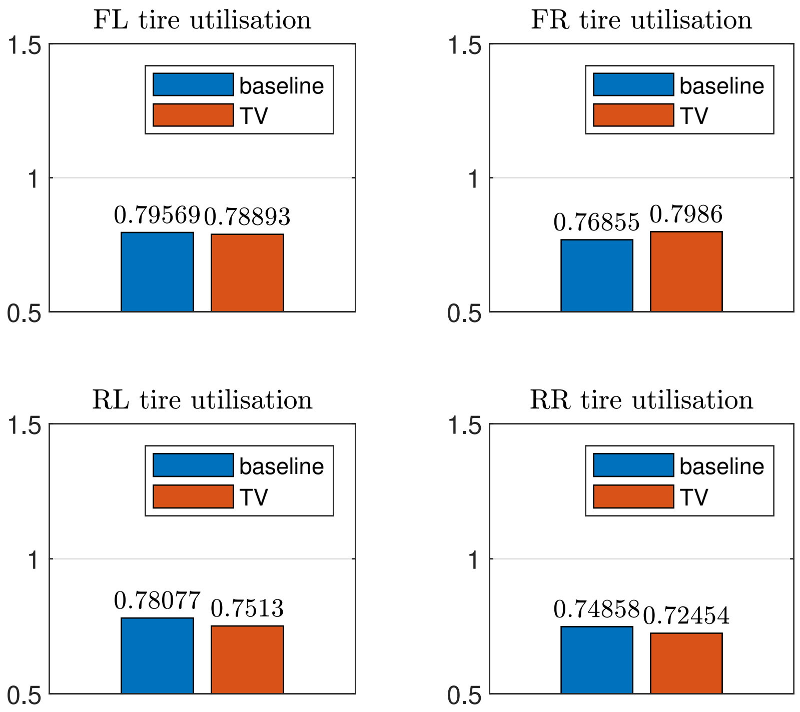

Figure 5.6: Tire utilisation of TV on endurance

Configuration	Time	Average Acceleration	Average speed	Points
baseline	65.88 s	11.85 m/s^2	16.50 m/s	113.15
TV	62.64 s	11.91 m/s^2	17.25 m/s	152.58
ΔTV	-3.23 s	0.06 m/s^2	0.75 m/s	39.43

Table 5.5: Time comparison baseline and TV on endurance

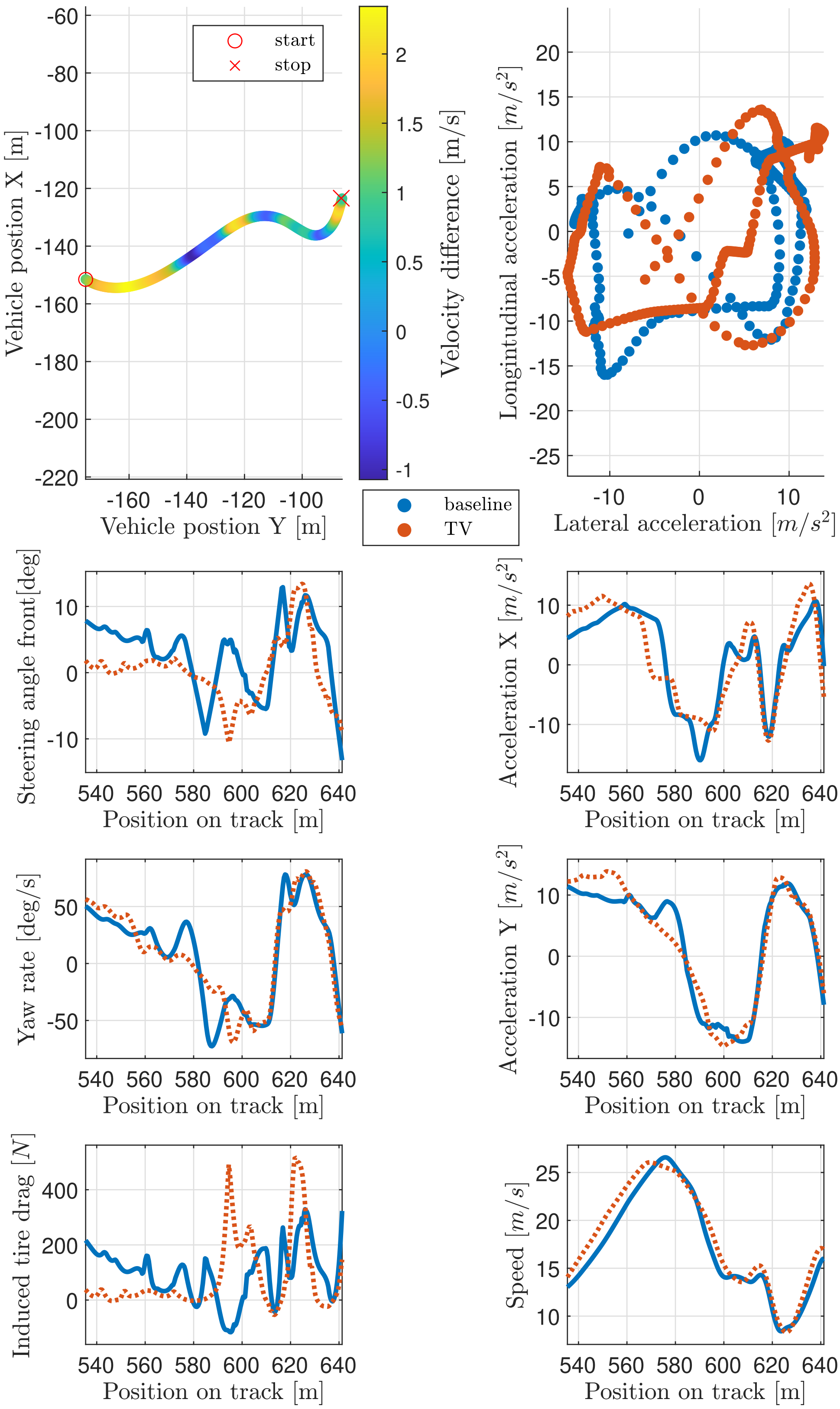

Figure 5.7: TV endurance analysis

5.2 Impact of RS on lap-time

Steering of rear wheels was limited to 6 degrees as per Formula Student rules. The impact of rear wheel steering has been evaluated by comparing baseline and RS on all disciplines.

Vehicle	Acceleration	Skidpad	Autocross	Endurance	Overall
baseline	42.2	7.03	5.03	113.15	167.65
RS	42.2	12.64	23.82	149.35	228
ΔRS	0	5.61	18.79	36. 2	60.34

Table 5.6: Points comparison between RS and baseline

5.2.1 Impact of RS on skidpad

The interesting thing in Figure 5.9 is that RS has negative longitudinal acceleration, this is caused by the fact that a vehicle with rear steering can have non zero body slip and zero slip angle on all tires at the same time. Therefore, lateral and longitudinal accelerations are not the best measures to compare vehicles, a better comparison would be combined acceleration. Tire utilization in figure 5.9 of RS is slightly better than baseline but worse than the vehicle with TV.

Configuration	Time	Average Acceleration	Average speed	Points
baseline	5.06 s	11.87 m/s^2	9.53 m/s	7.3
RS	4.92 s	12.25 m/s^2	9.57 m/s	12.64
ΔRS	-0.14 s	-0.38 m/s^2	0.04 m/s	5.34

Table 5.7: Summary comparison baseline and RS on skidpad

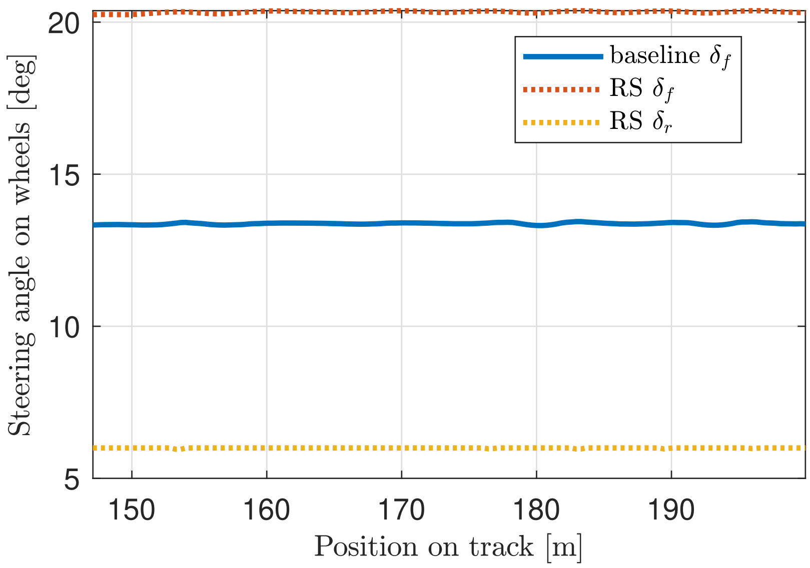

Figure 5.8: Steering angle of baseline and RS on skidpad

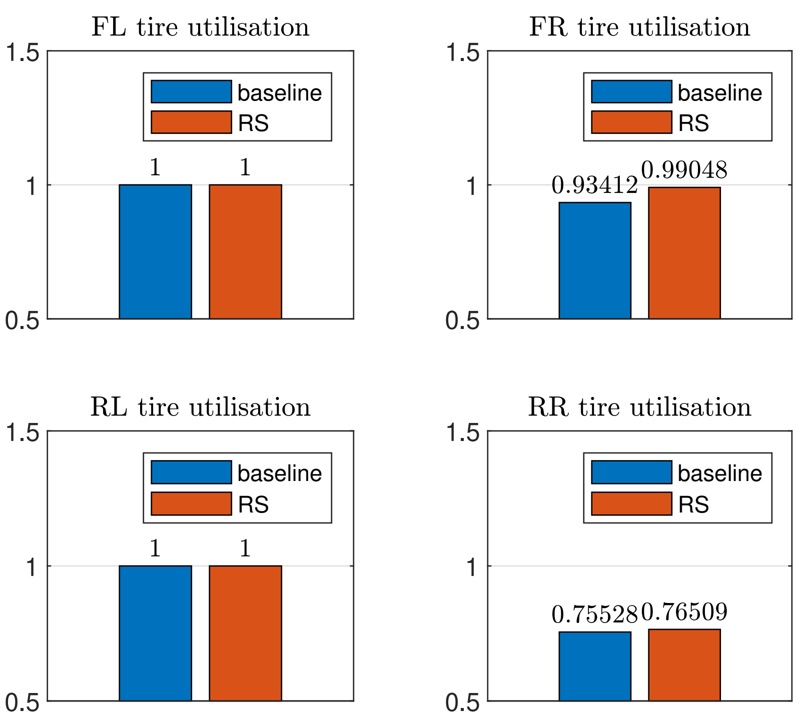

Figure 5.9: Tire utilization with rear steering on skidpad

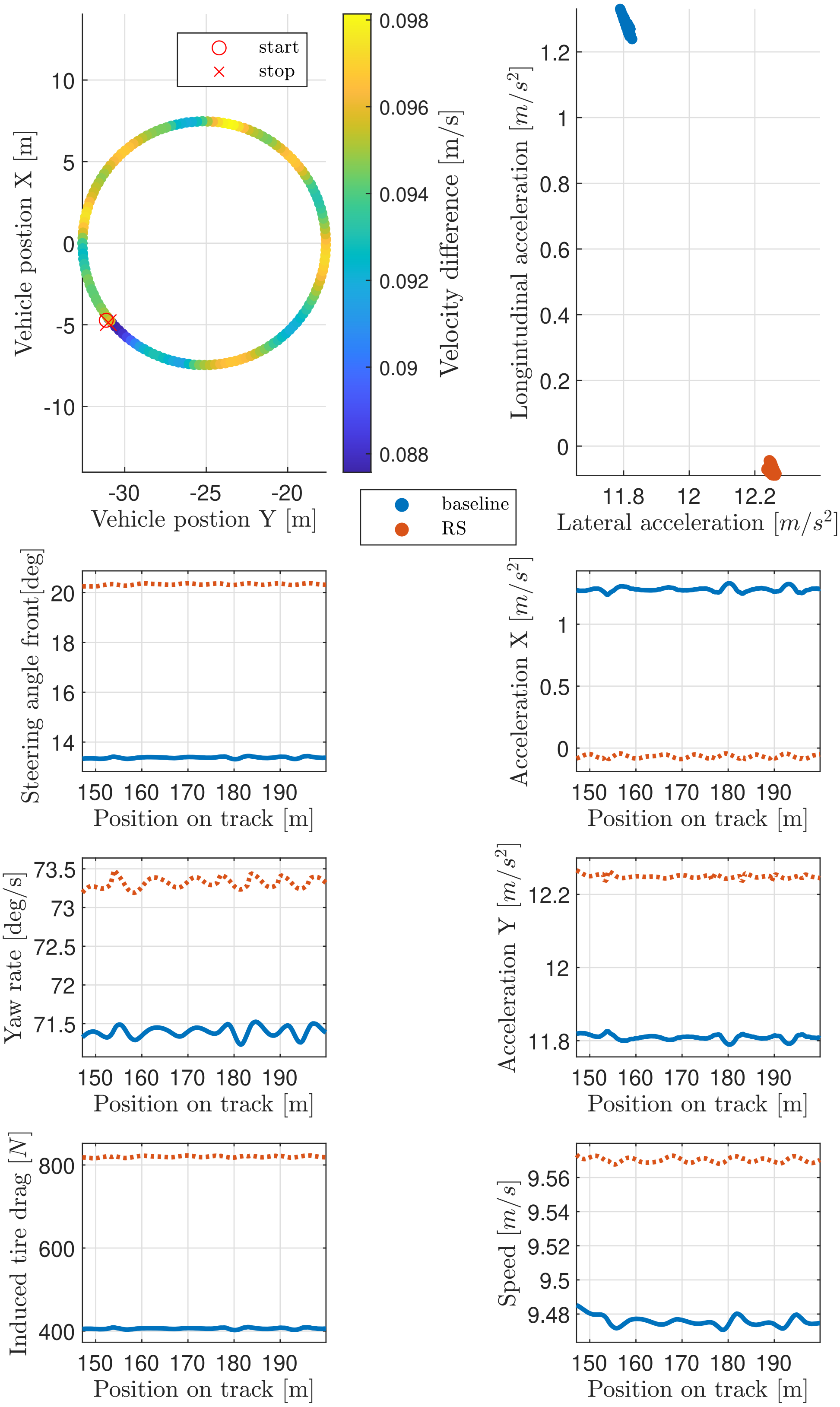

Figure 5.10: Rear steering skidpad analysis

5.2.2 Impact of RS on autocross

The impact of rear steering on autocross is very similar to the impact of TV regarding time. Times and points are in table 5.8. The rear steering allows higher speed on the entry of turn, whereas TV allows higher speed also on exit of the turn, this is shown on figures 5.13 and 5.5.

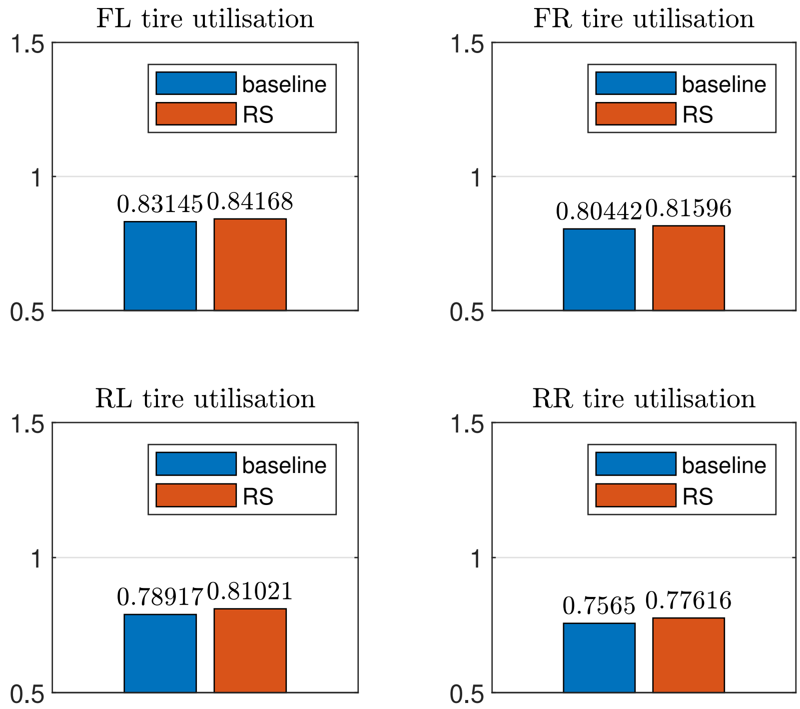

Figure 5.11: Tire utilisation with Rear steering on autocross

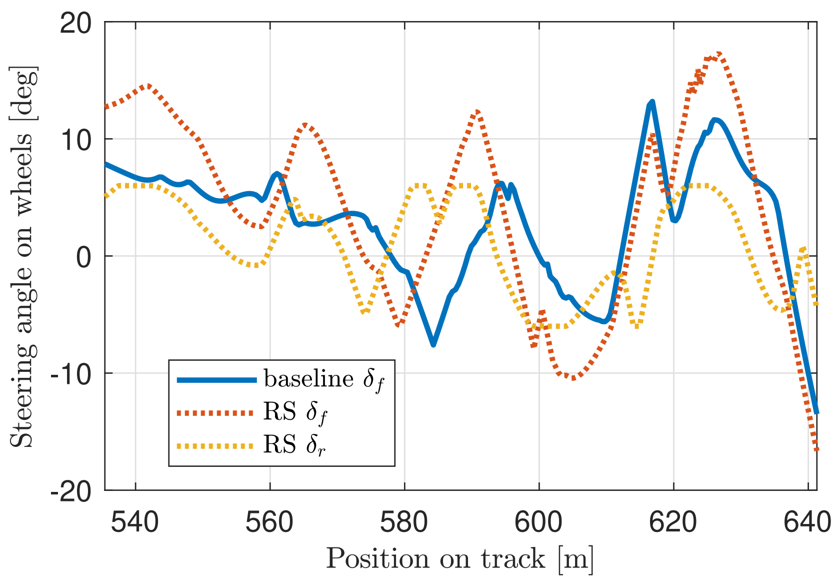

Figure 5.12: Rear steering autocross analysis

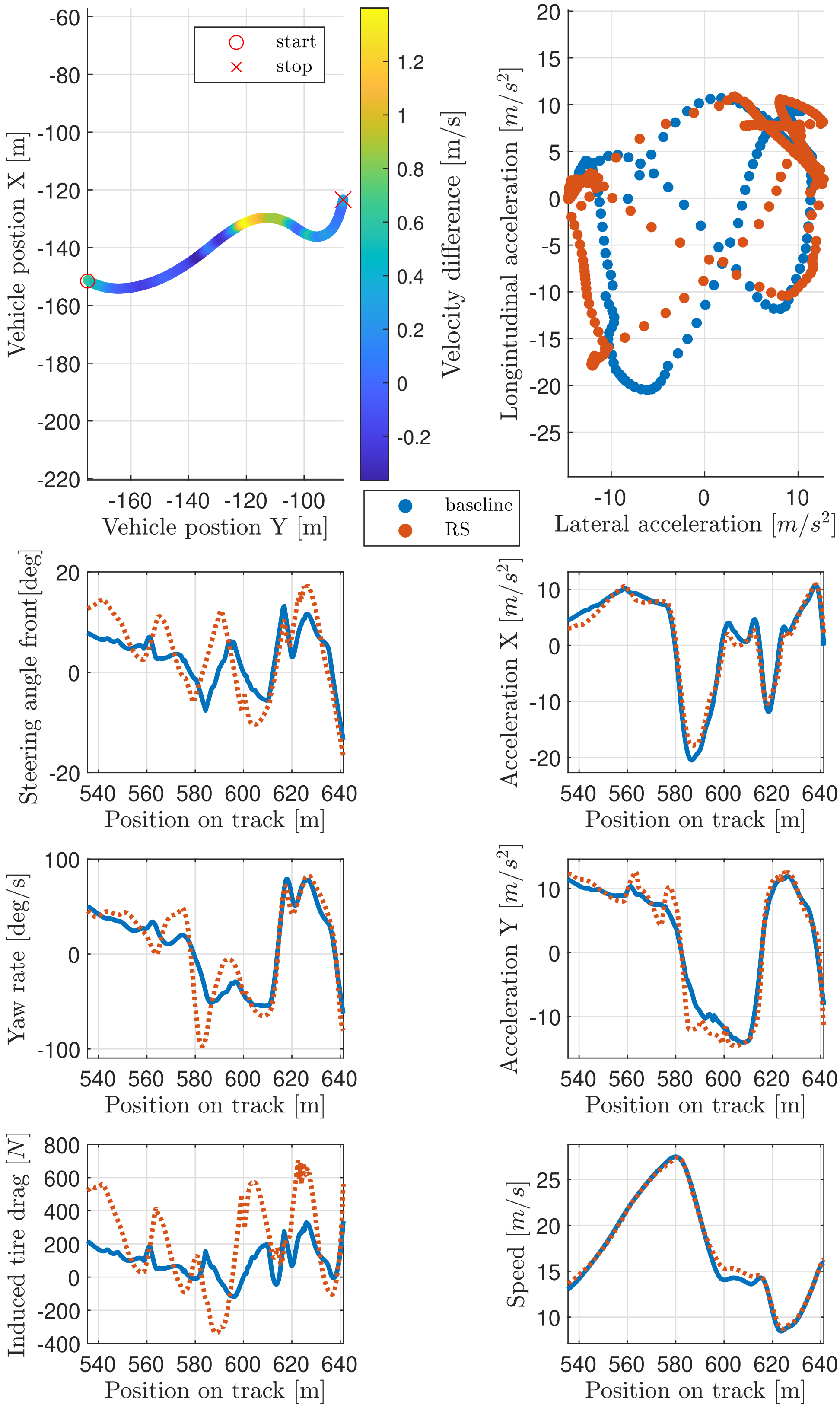

Figure 5.13: Rear steering autocross analysis

Configuration	Time	Average Acceleration	Average speed	Points
baseline	65.72 s	12.23 m/s^2	16.60 m/s	5.03
RS	62.66 s	12.68 m/s^2	17.24 m/s	23.82
ΔRS	-3.08 s	0.45 m/s^2	0.63 m/s	18.79

Table 5.8: Time comparison baseline and RS on autocross

5.2.3 Impact of RS on endurance

The impact of RS on endurance is also similar to that of TV. The comparison between baseline and RS is in table 5.9. Tire utilisation in figure 5.14 on rear wheels is lower than baseline and lap time is lower than baseline, this requires further investigation. Worth further analysis is also the tire induced drag which got to large negative values, which means the drag was accelerating the vehicle forward, this is shown in figure 5.15.

Configuration	Time	Average Acceleration	Average speed	Points
baseline	65.88 s	11.85 m/s^2	16.50 m/s	113.15
RS	62.90 s	12.02 m/s^2	17.06 m/s	149.35
ΔRS	-2.98 s	0.16 m/s^2	0.55 m/s	36.20

Table 5.9: Time comparison baseline and RS on endurance

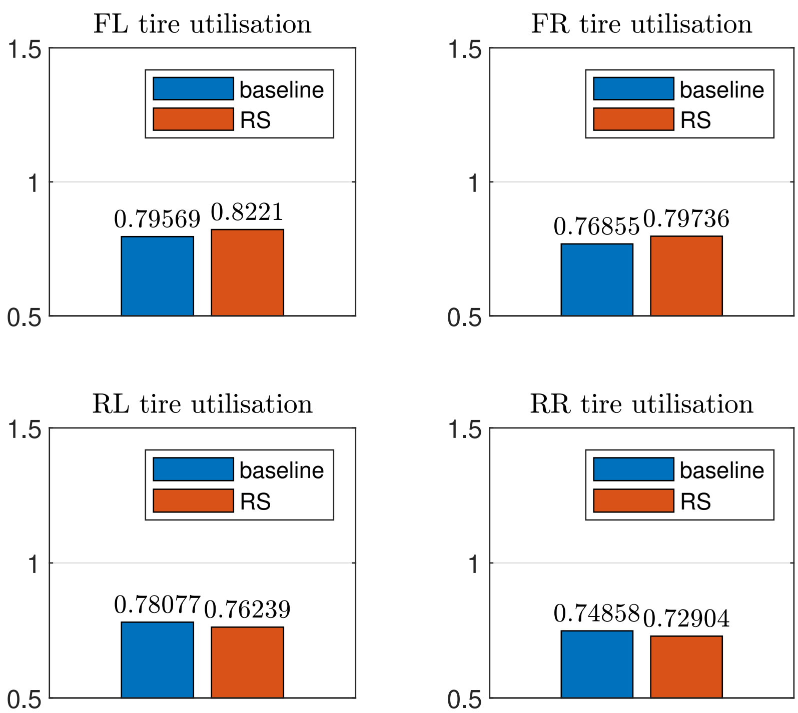

Figure 5.14: Tire utilisation with Rear steering on endurance

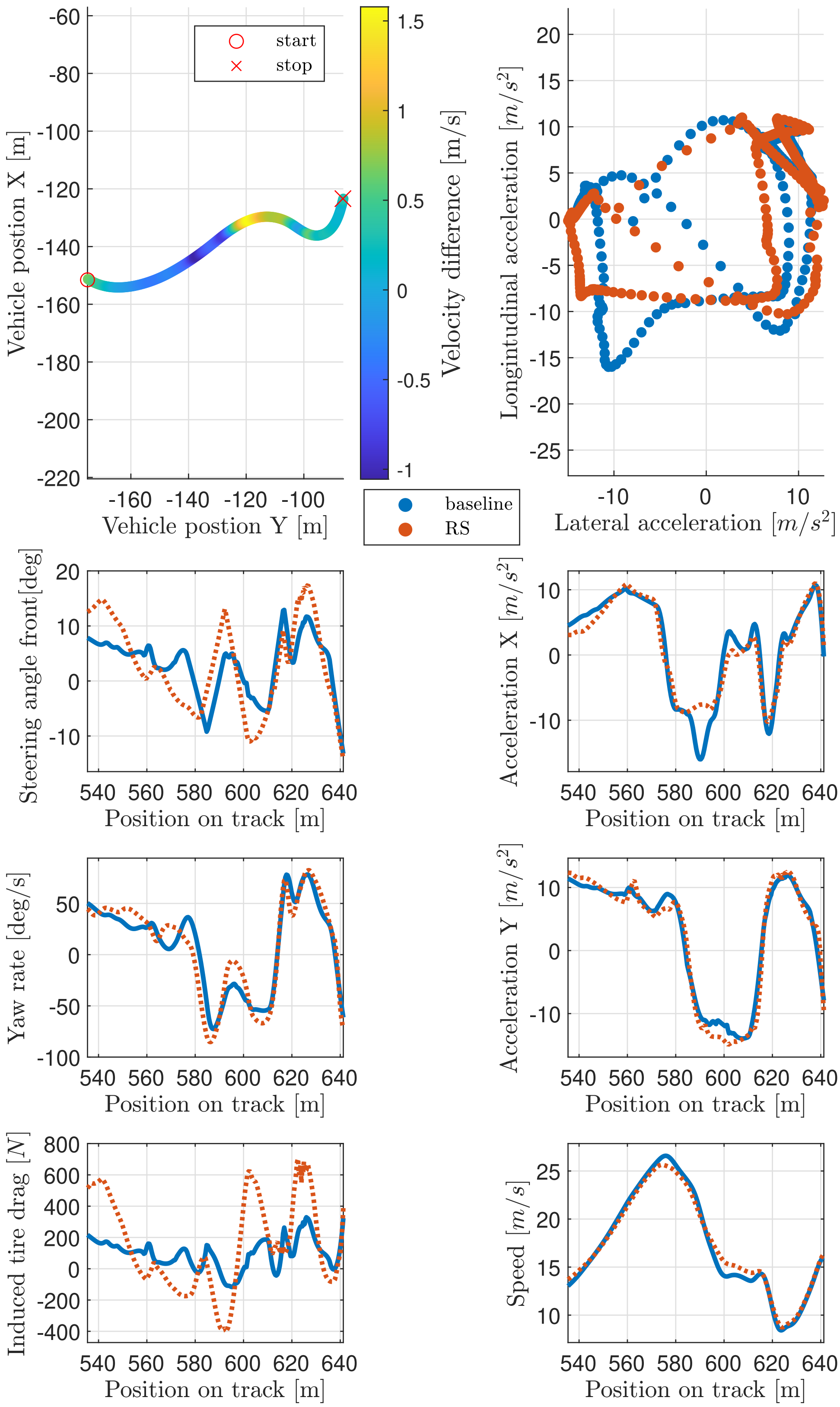

Figure 5.15: Rear steering endurance analysis

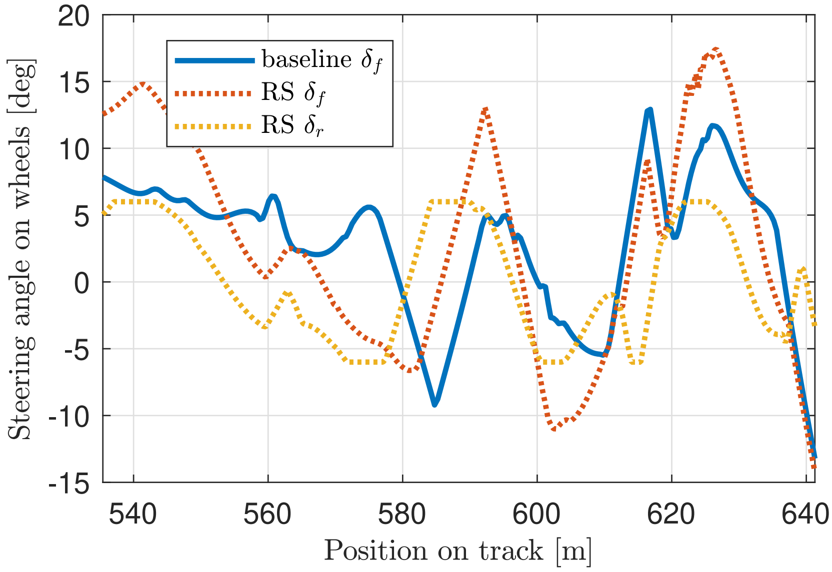

Figure 5.16: Rear steering endurance analysis

5.3 Impact of GEPD on lap-time

GEPD at full power creates additional normal force of 882 N, this system has its own separated accumulator and the whole system adds 10kg to the weight of the vehicle. The weight negatively impacts all disciplines, the GEPD accumulator can be fully discharged only during endurance. For other disciplines, GEPD is always on 100% power. GEPD is the only system examined that influences acceleration. Contrary to other systems, GEPD doesn't increase the utilization of the tire, but it increases the maximum forces the tire can sustain. Points comparison between baseline and GEPD vehicle is on table 5.10

Vehicle	Acceleration	Skidpad	Autocross	Endurance	Overall
baseline	42.2	7.03	5.0324	113.15	167.65
GEPD	45.56	33.77	54.44	157.47	291.26
ΔGEPD	3.36	26.74	49.40	44.32	123.61

Table 5.10: Points comparison between baseline and GEPD

5.3.1 Impact of GEPD on skidpad

GEPD has by far the highest impact on skipad time among other systems. The average acceleration on the skidpad has been increased by 3.52 m/s^2. Speed compared to baseline is 1.35 m/s higher, this is shown in figure 5.18 and table 5.11. Tire utilisation in figure 5.17 has changed insignificantly.

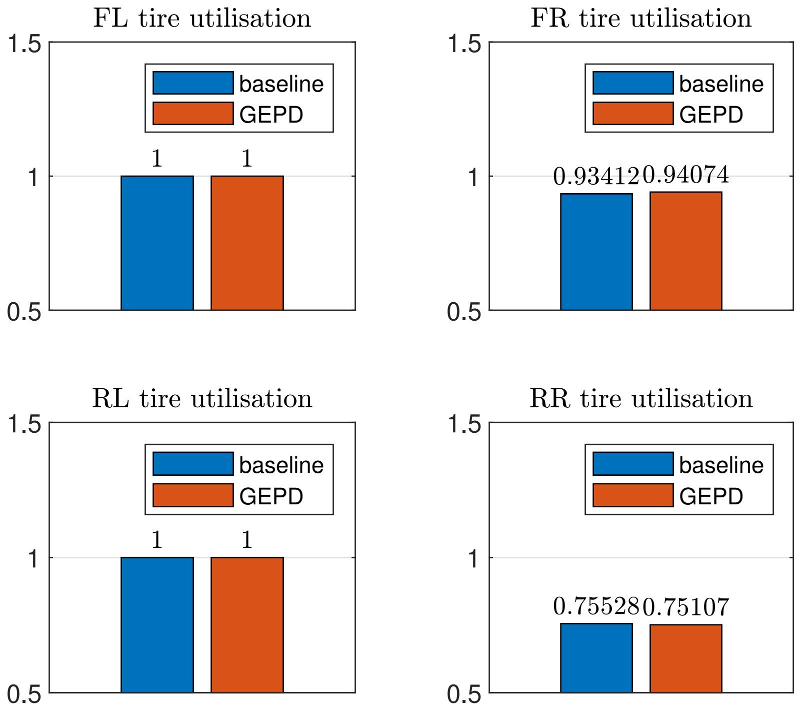

Figure 5.17: Tire utilization with GEPD on skidpad

Configuration	Time	Average Acceleration	Average speed	Points
baseline	5.06 s	11.87 m/s^2	9.5316 m/s	7.3
GEPD	4.43 s	15.5 m/s^2	10.89 m/s	33.78
ΔGEPD	-0.63 s	3.52 m/s^2	1.35 m/s	26.48

Table 5.11: Time comparison baseline and GEPD on skidpad

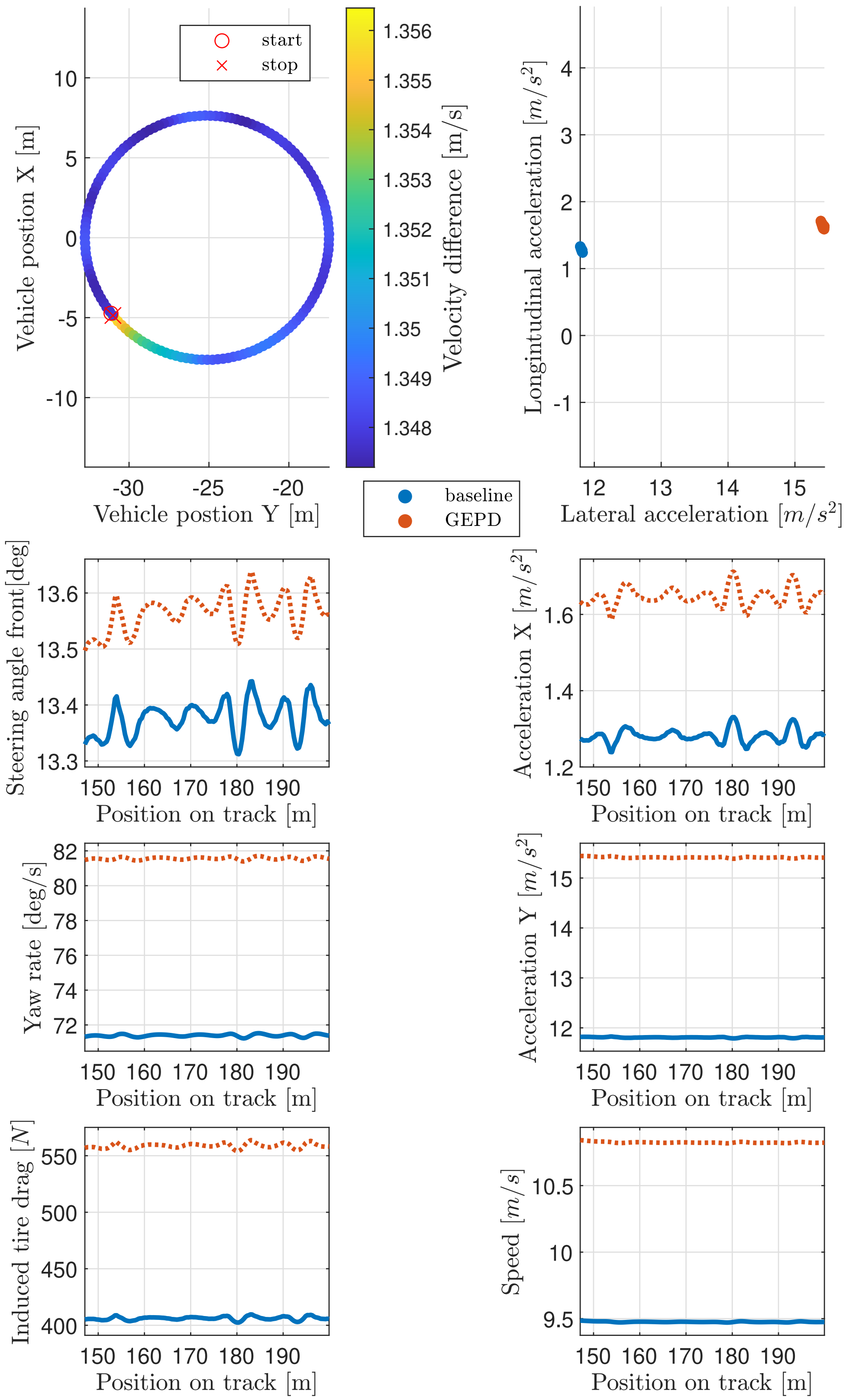

Figure 5.18: GEPD skidpad analysis

5.3.2 Impact of GEPD on autocross

Tire utilisation has significantly decreased with the GEPD system, see figure 5.19. Average acceleration on autocross has increased and average speed has also increased, see table 5.12.

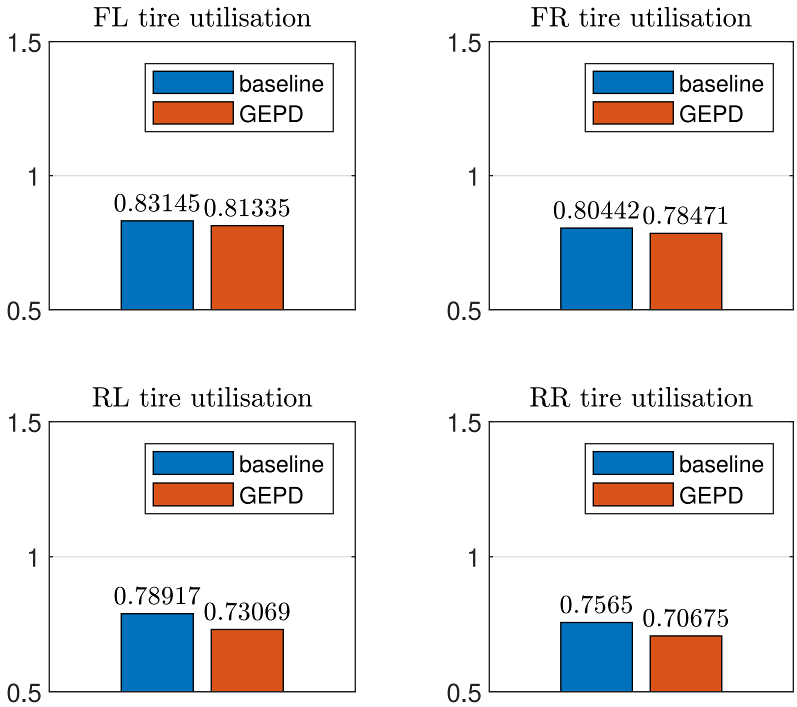

Figure 5.19: Tire utilization with GEPD on autocross

Configuration	Time	Average Acceleration	Average speed	Points
baseline	65.88 s	11.85 m/s^2	16.50 m/s	113.15
GEPD	62.9 s	12.02 m/s^2	17.06 m/s	149.35
ΔGEPD	-2.981 s	0.16 m/s^2	0.55 m/s	36.2

Table 5.12: Time comparison baseline and GEPD on autocross

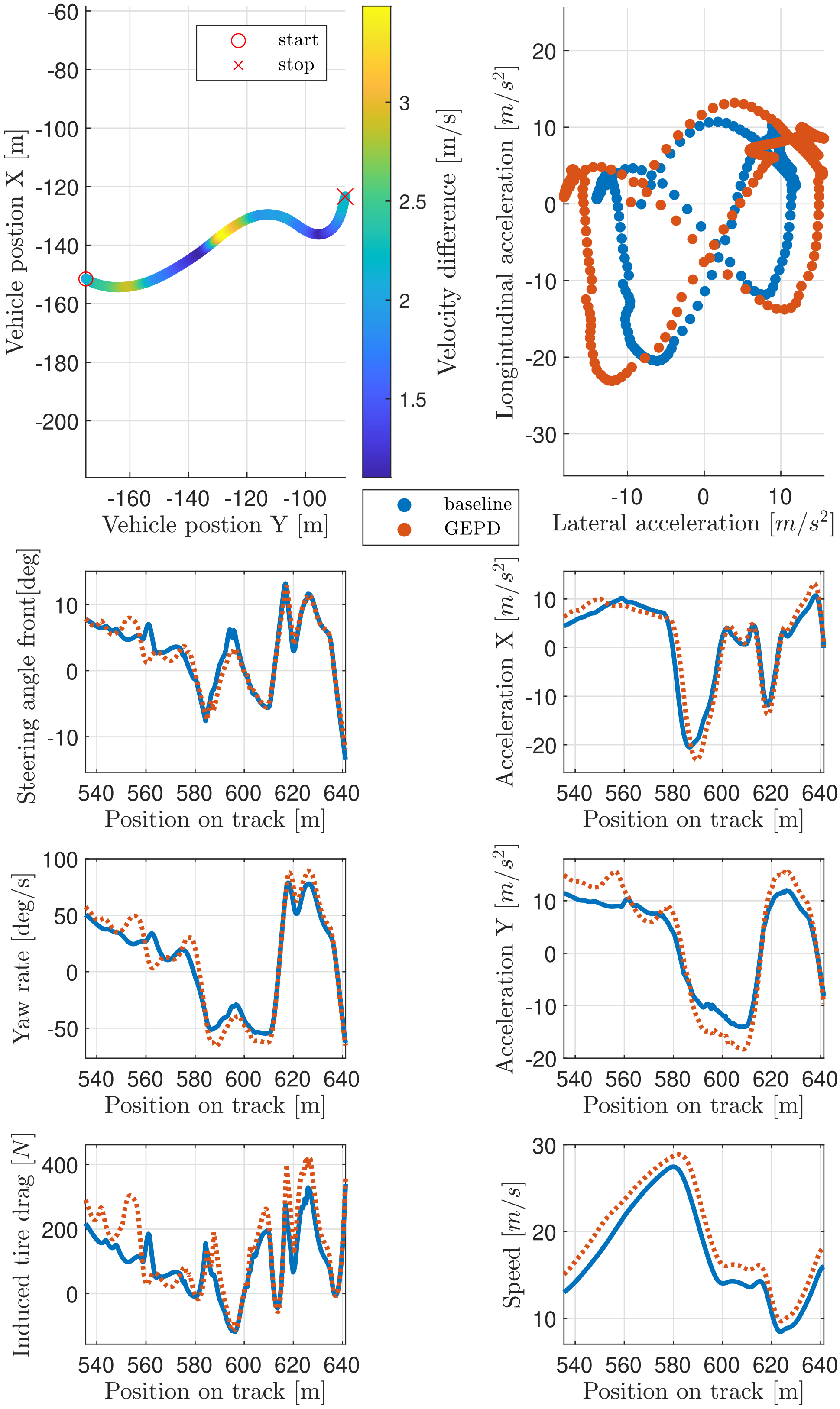

Figure 5.20: GEPD autocross analysis

5.3.3 Impact of GEPD on endurance

Vehicle with GEPD was on average faster than the baseline vehicle, however, figure 5.22 shows that the top speed at track position 575 m was lower than the baseline vehicle. GEPD could not run at 100% due to limited accumulator capacity. Figure 5.23 shows how GEPD was used during the track segment.

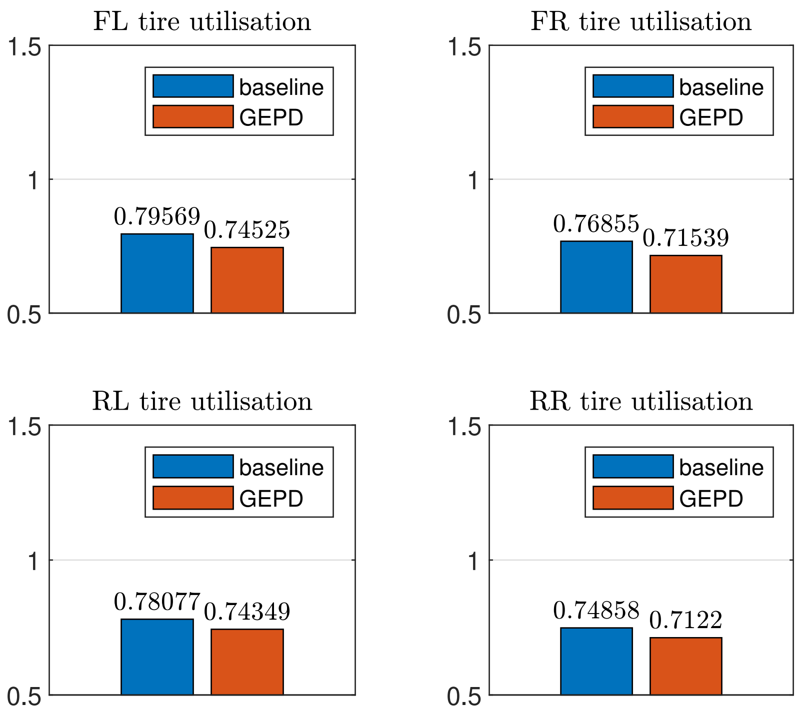

Figure 5.21: Tire utilization with GEPD on endurance

Configuration	Time	Average Acceleration	Average speed	Points
baseline	65.88 s	11.85 m/s^2	16.50 m/s	113.15
GEPD	62.26 s	12.219 m/s^2	17.08 m/s	157.47
ΔGEPD	-3.61 s	0.36 m/s^2	0.75 m/s	44.32

Table 5.13: Time comparison baseline and GEPD on endurance

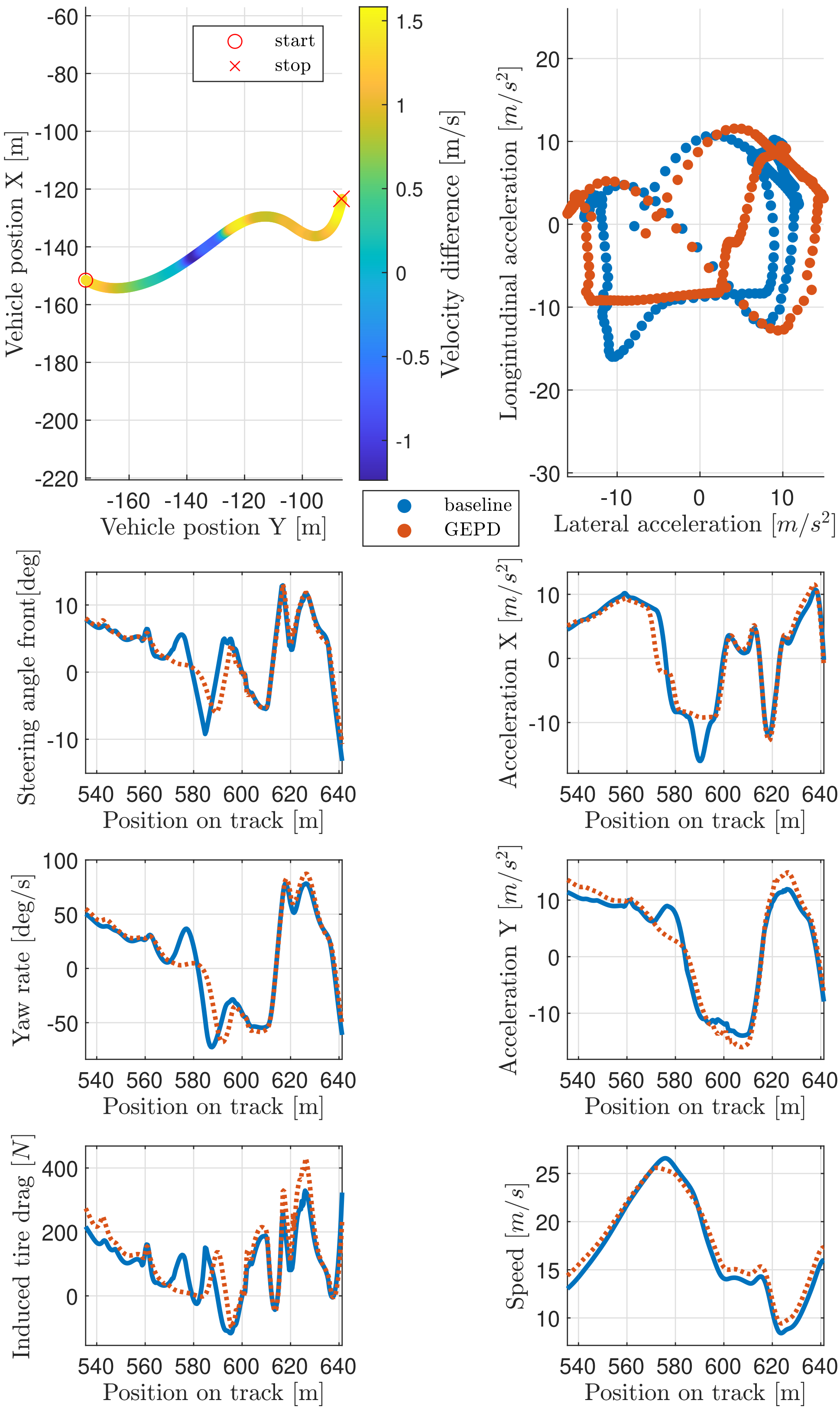

Figure 5.22: GEPD endurance analysis

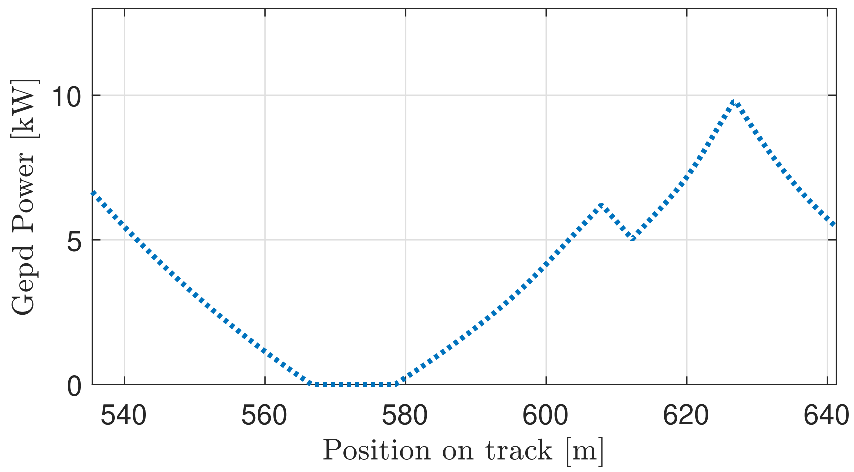

Figure 5.23: GEPD endurance analysis

5.4 Summary comparison

Figures 5.24 and 5.25 give a better overview of how systems improved the vehicle performance than previous graphs. Previous graphs only looked at a small portion of the track. These graphs compare the systems across the whole endurance discipline.

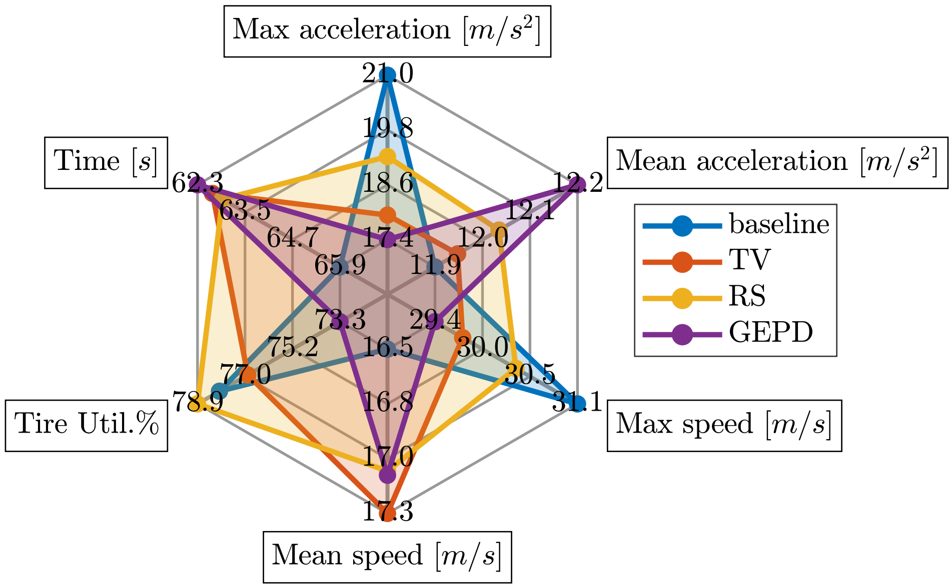

Figure 5.24: Driving quantities endurance

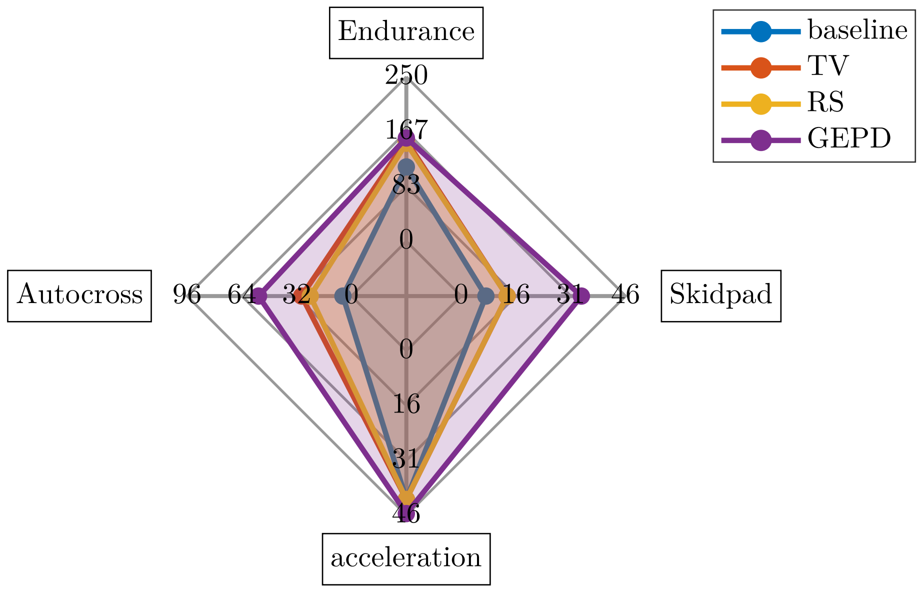

Figure 5.25: Points of each vehicle variant

5.5 Results verification

Verification has been done on the CarMaker CTU24 model. Controls calculated by the optimization framework have been fed into the carmaker model. To ensure that the differences in models do not cause the car to stray off-path, a feedback path keeping control from the carmaker has been used. The Carmaker model is then controlled by the feed-forward method (precomputed controls from optimization) and feedback method (carmaker). Diagram of the controller is on figure 5.26 Verification is not supposed to verify the on limit behavior of the CarMaker model, it verifies that controls obtained from optimisation framework can be used to drive a vehicle without a major intervention of the feedback controller. For the purpose of verification, the forces from the twin track tire model have been lowered by 30% to ensure the CarMaker model will stay within its limits. Verification has been performed on the baseline and TV vehicle on the autocross track. Table 5.14 shows times calculated by the optimization framework and times that the CarMaker returned after running the verification simulation. Figure 5.27 shows the steering angle at the front wheels taken from verification in CarMaker. The maximum steering angle from the controller is 5 degrees, which is substantial when compared to the maximum steering used from the optimization framework, which is 15 degrees.

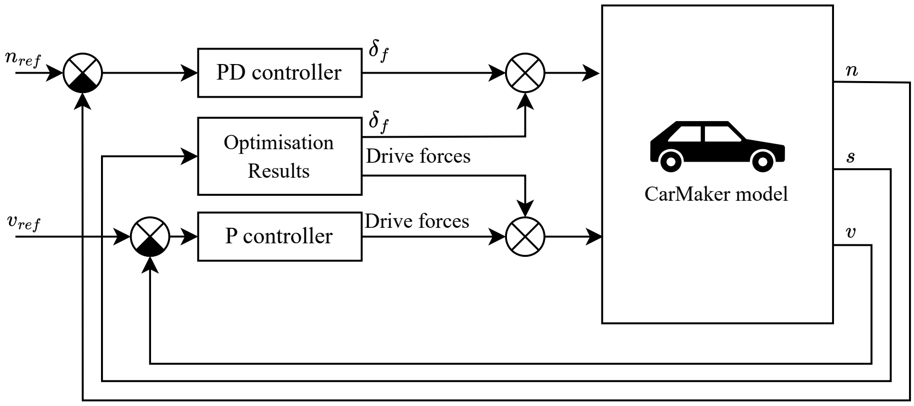

Figure 5.26: Verification diagram

	baseline	TV
Time from optimisation	77.39	73.71
Time from verification	76.02	72.10
TimeΔ	-1.37	-1.61

Table 5.14: Verification lap times

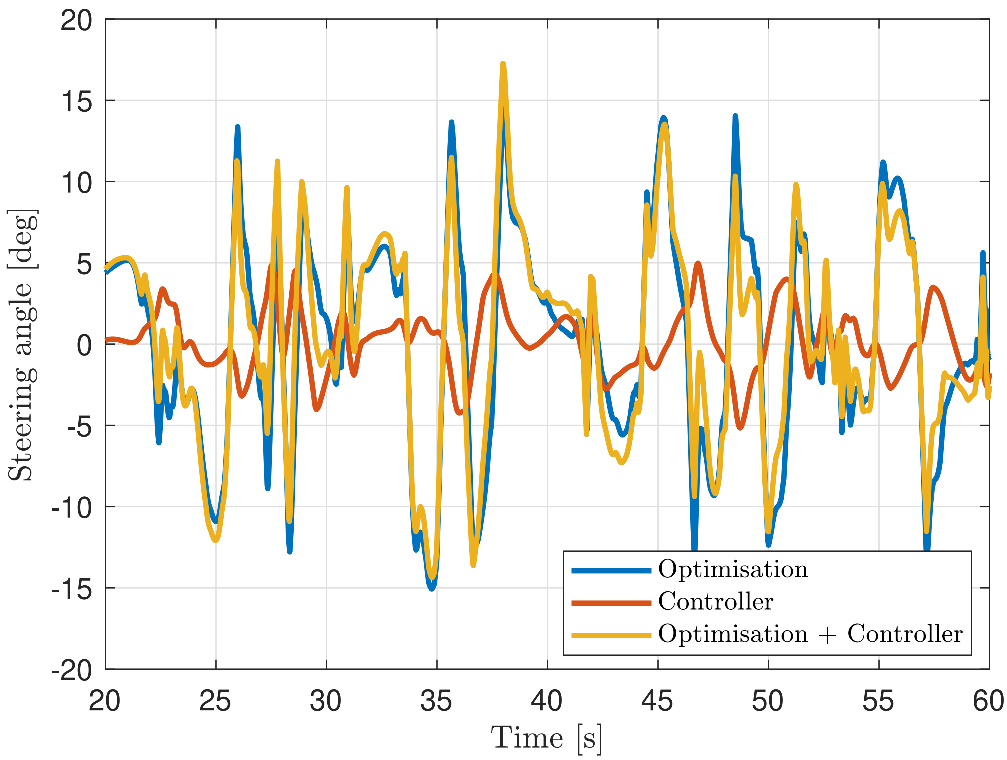

Figure 5.27: Verification comparison

Chapter 6

Conclusion

In conclusion, the model of the formula student vehicle was created with sufficient fidelity and validated with reality and high-fidelity simulation software CarMaker. Validation was only done for ramp steer, this maneuver does not capture the dynamics of the vehicle. To capture dynamics a step steer maneuver should be validated too. The optimization framework was augmented with a validated twin track model, a more refined tire model, aerodynamic effects, power limitation, mechanical braking, power losses, suspension model, and GEPD model. Four vehicle configurations were created: baseline, TV, RS and GEPD. Simulation of Formula Student Czech 2023 was done for each of the vehicle configurations to evaluate the time and point gain of each of the systems, that is 16 simulations. Verification of simulation output was done on 2 out of 16 simulations. Verification showed moderate fit with CarMaker, the maximum output of the controller was 5 degrees and the maximum steering angle of the vehicle was 15.

Furthermore, tire model could be improved by using the Magic Formula model[3]. Wheel spin and slip ratio can be also implemented. The suspension model can be improved by replacing the 1-st order system with a stiffness and damping model for roll, pitch and heave. The current model does not consider any change in elevation of the track. Adding this would also bring the model closer to reality.

More analysis is needed, in order to find out the exact mechanism the systems are improving the vehicle performance . Sensitivity analysis of vehicle parameters should be performed using this tool. The current computation time for endurance discipline is around 4 hours, settings of Ipopt should be investigated as well as the formulation of constraints to reduce the computation time.

Acronyms

DOF Degree of Freedom. 2

FSAE Formula Student Society of Automobile Engineers. 12

FSCZ Formula Student Czech Republic. vi, 9, 10

GEPD Ground Effect Production Device. vi, vii, 1, 13, 17, 22, 24, 43, 47

Ipopt Interior Point Optimizer. iv, 23, 26, 53

MLTS Minimum lap time simulation. 2, 12

RS Rear Wheels Steering. vii, 27, 35, 40, 53

TTC Tire Testing Consortium. 12

TV Torque Vectoring. vi, vii, 2, 27–29, 31, 38

Bibliography

[1] Joel A E Andersson, Joris Gillis, Greg Horn, James B Rawlings, and Moritz Diehl. CasADi – A software framework for nonlinear optimization and optimal control. *Mathematical Programming Computation*, 11(1):1–36, 2019.

[2] A. Wächter and L.T. Biegler. On the implementation of an interior-point filter line-search algorithm for large-scale nonlinear programming. *Mathematical Programming, 106(1):25–57*, 2006.

[3] Hans B Pacejka. *Tire and Vehicle Dynamics*. Butterworth-Heinemann, 2012.

[4] Scherenberg H. Mercedes-benz racing design and cars experience. *SAE Transactions*, 1958.

[5] Matteo Massaro and David Limebeer. Minimum-lap-time optimisation and simulation. *Vehicle System Dynamics*, 59:1–45, 04 2021.

[6] Thelin CF Roland RD. Computer simulation of watkins glen grand prix circuit performance. *Cornell Aeronautical Laboratory*, 1971.

[7] Steven De Groote. The vehicle performance envelope.

[8] Kimura T Fujioka T. Numerical simulation of minimum-time cornering behavior. *JSAE review*, 1992.

[9] Kriens RFC Hendrikx JPM, Meijlink TJJ. Application of optimal control theory to inverse simulation of car handling. *Vehicle System Dynamics*, 1996.

[10] Symonds P Casanova D, Sharp RS. Minimum time manoeuvring: The significance of yaw inertia. *Vehicle System Dynamics*, 2000.

[11] Gadola M Dal Bianco N, Lot R. Minimum time optimal control simulation of a gp2 race car. *Proceedings of the Institution of Mechanical Engineers, Part D: Journal of Automobile Engineering*, 2018.

[12] Arajo RE De Castro R, Tanelli M. Minimum-time manoeuvring in electric vehicles with four wheel-individual-motors. *Vehicle System Dynamics*, 2014.

[13] Optimumlap. `https://students.optimumg.com/product/optimumlap/`. Accessed: 2024-02-5.

[14] Yukio Nakajima. *Advanced Tire Mechanics*, pages 707–710. Springer, 2019.

[15] Suspension secrets. `https://suspensionsecrets.co.uk/camber/`. Accessed: 2024-02-5.

[16] Fsae tire test consortium. `https://www.millikenresearch.com/fsaettc.html`. Accessed: 2024-02-5.

[17] Lord Rayleigh. Liii. on the resistance of fluids. *The London, Edinburgh, and Dublin Philosophical Magazine and Journal of Science*, 2(13):430–441, 1876.

[18] Load transfer. `https://optimumg.com/load-transfer/`. Accessed: 2024-02-5.

[19] Giacomo Perantoni and David J. N. Limebeer. Optimal control for a formula one car with variable parameters. *Vehicle System Dynamics*, 2014.